

SYNTHESIS OF TOPOISOMERASE INHIBITOR TYPE ANTICANCER DRUGS  
LINKED GOLD NANOPARTICLES

A THESIS SUBMITTED TO  
THE GRADUATE SCHOOL OF NATURAL AND APPLIED SCIENCES  
OF  
MIDDLE EAST TECHNICAL UNIVERSITY

BY

GÖNÜL PEKÇAĞLIYAN

IN PARTIAL FULFILLMENT OF THE REQUIREMENT  
FOR  
THE DEGREE OF MASTER OF SCIENCE  
IN  
CHEMISTRY

JANUARY 2008

Approval of the thesis:

**SYNTHESIS OF TOPOISOMERASE INHIBITOR TYPE ANTICANCER  
DRUGS LINKED GOLD NANOPARTICLES**

submitted by **GÖNÜL PEKÇAĞLIYAN** in partial fulfillment of the requirements  
for the degree of **Master of Science in Chemistry Department, Middle East  
Technical University** by,

Prof. Dr. Canan Özgen  
Dean, Graduate School of **Natural and Applied Sciences**

\_\_\_\_\_

Prof. Dr. Ahmet M. Önal  
Head of Department, **Chemistry**

\_\_\_\_\_

Prof. Dr. Ayhan S. Demir  
Supervisor, **Chemistry Dept., METU**

\_\_\_\_\_

**Examining Committee Members:**

Prof. Dr. Bekir Peynircioğlu  
Chemistry Dept., METU

\_\_\_\_\_

Prof. Dr. Ayhan S. Demir  
Chemistry Dept., METU

\_\_\_\_\_

Prof. Dr. Metin Zora  
Chemistry Dept., METU

\_\_\_\_\_

Assoc. Prof. Dr. Özdemir Doğan  
Chemistry Dept., METU

\_\_\_\_\_

Assist. Prof. Dr. Nezire Saygılı  
Pharm. Dept., Hacettepe Univ.

\_\_\_\_\_

**Date:** January 21, 2008

**I hereby declare that all information in this document has been obtained and presented in accordance with academic rules and ethical conduct. I also declare that, as required by these rules and conduct, I have fully cited and referenced all material and results that are not original to this work.**

Name, Last name: Gönül PEKÇAĞLIYAN

Signature :

## ABSTRACT

### SYNTHESIS OF TOPOISOMERASE INHIBITOR TYPE ANTICANCER DRUGS LINKED GOLD-NANOPARTICLES

Pekçağlıyan, Gönül

MS, Department of Chemistry

Supervisor: Prof. Dr. Ayhan S. Demir

January 2008, 64 pages

This study presents studies on camptothecin (CPT), a potent antitumor agent in order to improve its stability and solubility without reducing its activity. The work describes the modification of camptothecin at 20-OH position a new strategy to overcome the stability and solubility problems of the free drug. Camptothecin is connected to linker that could be processed to a terminal thiol group and this thiol group was connected to gold surface, to obtain CPT-gold nanoparticles.

In the first part of the study; undecenol was chosen as the starting material and reacted with azobisisobutyronitrile to obtain S-11-hydroxyundecyl ethanethioate. 11-hydroxyundecyl ethanethioate was reacted with NaOMe to synthesize the target linker 11, 11'-disulfanediyldiundecan. After synthesis of the target linker, the 20-OH functional group of CPT was replaced with this linker to obtain 20- (11, 11'-disulfanediyldiundecan) - camptothecin.

The second part of the study, gold nanoparticles were synthesized by using  $\text{HAuCl}_4$  solution and the camptothecin derivative containing thiol group at 20-OH position was connected to the gold surface.

Keywords: Camptothecin, gold nanoparticles, prodrug

## ÖZ

### TOPOİZOMERAZ İNHİBİTÖRÜ ANTİKANSER İLAC- ALTIN NANOPARÇACIKLARIN SENTEZLERİ

Pekçağlıyan, Gönül

Yüksek Lisans, Kimya Bölümü

Tez Yöneticisi: Prof. Dr. Ayhan S. Demir

Ocak 2008, 64 sayfa

Bu çalışma serbest ilacın stabilite ve çözünürlük problemlerini çözmek için yeni bir strateji olan kamptotesinin 20-OH pozisyonundan modifikasyonunu içermektedir ve topoizomeraz inhibitörü türünde antikanser ilaç uç kısmı tiyol grubu içeren bağlayıcı gruplara eklenmiş ve tiyol grupları altın yüzeyine bağlanmıştır.

Çalışmanın ilk bölümünde, undekanol başlangıç maddesi olarak seçildi ve azobisizobutilnitril ile reaksiyonu sonucu 11-hidroksiundekil etantiyoat sentezlenmiştir. 11-hidroksiundekil etantiyoat NaOMe ile reaksiyona sokularak hedeflenen linker 11, 11'-disulfandiildiundekan elde edilmiştir. Bu linker kamptotesin ile reaksiyona sokularak - (11, 11'- disulfandiildiundekan) – kamptotesin elde edilmiştir.

Çalışmanın ikinci bölümünde ise, altın nanoparçacıkları  $\text{HAuCl}_4$  çözeltisi kullanılarak sentezlenmiş ve 20-OH pozisyonunda tiyol grubu içeren kamptotesin türevi altın yüzeyine bağlanmıştır.

Anahtar kelimeler: Kamptotesin, altın nanoparçacık, ön ilaç

*To My Father*

## ACKNOWLEDGEMENTS

I would like to express my deepest gratitude to my supervisor Prof. Dr. Ayhan Sitki Demir for his guidance, advice, criticism and encouragement throughout this research.

I wish to thank to my family for their love, encouragement, understanding and every thing they did for me.

Very special thanks to Eser Pirkin for his endless help, understanding , friendship and moral support. It was great for me to work with him at the same laboratory.

My special appreciation goes to Hamide Fındık who helped me very much for writing this thesis and also thanks for her indispensable friendship.

I wish to thank Demir's group members, for help, discussion, and the time we shared together.

Finally, I am grateful to Fatos D. Polat and Seda Karayılan for their great support for the NMR spectra and their interpretations.

## TABLE OF CONTENTS

ABSTRACT.....	iv
ÖZ.....	v
DEDICATION.....	vi
ACKNOWLEDGEMENTS.....	vii
TABLE OF CONTENTS.....	viii
LIST OF FIGURES.....	x
LIST OF ABBREVIATIONS.....	xii

## CHAPTERS

<b>1. INTRODUCTION.....</b>	<b>1</b>
<b>1.1. Cancer.....</b>	<b>1</b>
<b>1.2. Capmtothecin.....</b>	<b>2</b>
<b>1.2.1 DNA Topoisomerases.....</b>	<b>6</b>
<b>1.2.2 Camptothecins as Topoisomerase Poisons: Mechanism of Action.....</b>	<b>10</b>
<b>1.2.3 Structural Models for the Ternary Cleavable Complex Formed Between Human Topo I, DNA, and CPT.....</b>	<b>11</b>
<b>1.3. Nanotechnology and Nanomedicine.....</b>	<b>14</b>
<b>1.3.1. Nanomedicine.....</b>	<b>16</b>
<b>1.3.1.1. Immunoisolation.....</b>	<b>16</b>
<b>1.3.1.2. Gated nanosieves.....</b>	<b>17</b>
<b>1.3.1.3. Superparamagnetic nanoparticles.....</b>	<b>18</b>
<b>1.3.1.4. Ultrafast DNA Sequencing.....</b>	<b>19</b>
<b>1.3.1.5. Fullerene-Based Pharmaceuticals.....</b>	<b>19</b>
<b>1.3.1.6. Liposomes.....</b>	<b>20</b>
<b>1.3.1.7. Nanoshells.....</b>	<b>20</b>
<b>1.3.1.8. Dendrimers.....</b>	<b>21</b>
<b>1.3.2. Gold Nanoparticles.....</b>	<b>22</b>
<b>1.4. Aim of the Work.....</b>	<b>23</b>

<b>2.RESULTS &amp; DISCUSSION</b> .....	25
<b>2.1. Modifications in E Ring</b> .....	25
<b>2.2. Synthesis of 20-(11, 11'-disulfaneyldiundecan)</b>	
- Camptothecin Derivative.....	29
<b>2.2.1. First Applied Method for Synthesis of</b>	
20-(11, 11'-disulfaneyldiundecan) - Camptothecin Derivative.....	30
<b>2.2.2. Second Applied Method for Synthesis of</b>	
20-(11, 11'-disulfaneyldiundecan) - Camptothecin Derivative.....	32
<b>2.2.3. Third Applied Method for Synthesis of</b>	
20-(11, 11'-disulfaneyldiundecan) - Camptothecin Derivative.....	34
<b>2.3. Synthesis of Gold Nanoparticles and 20-(11, 11'-disulfaneyldiundecan) –</b>	
camptothecin Derivative coated Gold Nanoparticles.....	40
<b>3. EXPERIMENTAL</b> .....	47
<b>3.1. General Procedure for the Synthesis of</b>	
S-11-hydroxyundecyl ethanethioate (6).....	48
<b>3.2. General Procedure for the Synthesis of</b>	
11,11'-disulfaneyldiundecan-1-ol (7).....	48
<b>3.3. General Procedure for the Synthesis of</b>	
20-( undec-10-en)- camptothecin (16).....	48
<b>3.4. General Procedure for the Synthesis of</b>	
20-( S-11-hydroxyundecyl ethanethioate)- camptothecin (17).....	49
<b>3.5. General Procedure for the Synthesis of</b>	
20-( 11,11'-disulfaneyldiundecan)- camptothecin (8).....	49
<b>3.6. General Procedure for the Synthesis 20-(11, 11'-disulfaneyldiundecan) –</b>	
camptothecin coated Gold Nanoparticles .....	50
<b>4.CONCLUSION</b> .....	51
<b>5. REFERENCES</b> .....	52
<b>6.APPENDIX</b> .....	59

## LIST OF FIGURES

<b>Figure 1.</b> Structure of Camptothecin .....	2
<b>Figure 2.</b> Camptothecin hydrolysis to water soluble sodium salt.....	4
<b>Figure 3.</b> Structure of topotecan.....	5
<b>Figure 4.</b> Structure of Irinotecan and SN38.....	6
<b>Figure 5:</b> Mechanism of Relaxation DNA by Topoisomerase I and Topoisomeras II.....	7
<b>Figure 6:</b> Mechanism of DNA relaxation by topoisomerase I.....	9
<b>Figure 7:</b> Mechanism of action of Camptothecin.....	11
<b>Figure 8:</b> Hol Base- Flipping Model.....	12
<b>Figure 9:</b> Pommier Intercalation Model.....	12
<b>Figure 10:</b> Kerrigan Intercalation Model.....	14
<b>Figure 11:</b> Relative sizes of small objects.....	16
<b>Figure 12.</b> Retrosynthetic analysis of modification of CPT from 20- OH position.....	24
<b>Figure 13.</b> Mechanism of camptothecin hydrolysis to water soluble sodium salt.....	26
<b>Figure 14.</b> Structures of CPT lactam and thiolactone.....	27
<b>Figure 15.</b> Structures of 20- aminoCPT, 20-deoxyCPT and halogenated CPTs.....	27
<b>Figure 16.</b> Structures of 20-O-linked nitrogen-based camptothecin ester derivatives and phosphonate analogs of CPT.....	28
<b>Figure 17:</b> Target Molecules.....	28
<b>Figure 18.</b> Reactions of CPT with different linkers.....	29
<b>Figure 19.</b> First planned retro-synthetic way for the synthesis of 20-OH substituted CPT derivative 30	
<b>Figure 20.</b> Synthesis of 20- (undec-10-en) camptothecin 31	
<b>Figure 21.</b> Second planned retro-synthetic way for the synthesis of 20-OH substituted CPT derivative 32	

<b>Figure 22.</b> Synthesis of 20-(S-11-hydroxyundecyl ethanethioate)camptothecin	33
<b>Figure 23.</b> Third planned retro-synthetic way for the synthesis of 20-OH substituted CPT derivative	35
<b>Figure 24.</b> Synthesis of 20- (11,11'-disulfanediyldiundecan)captothecin	
<b>Figure 25.</b> Percentage of lacton CPT and 20- (11, 11'-disulfanediyldiundecan) – captothecin graph	39
<b>Figure 26.</b> Synthesis of gold nanoparticles	41
<b>Figure 27.</b> Synthesis of 20-(11, 11'-disulfanediyldiundecan)- Camptothecin coated AuNPs	42
<b>Figure 28:</b> UV-VIS Spectrum of the Gold Nanoparticles	43
<b>Figure 29.</b> Percentage of lacton CPT and 20 - (11, 11'-disulfanediyldiundecan) – captothecin coated AuNPs graph	44
<b>Figure 30:</b> Confocal Microscopie Image of 20-(11'-disulfanediyldiundecan) – Camptothecin Coated Gold Nanoarticles	45
<b>Figure 31:</b> TEM Image of 20-(11'-disulfanediyldiundecan) – Camptothecin Coated Gold Nanoarticles	46
<b>Figure 30:</b> <sup>1</sup> H and <sup>13</sup> C NMR spectra of (6)	59
<b>Figure 31:</b> <sup>1</sup> H and <sup>13</sup> C NMR spectra of (7)	60
<b>Figure 32:</b> <sup>1</sup> H and <sup>13</sup> C NMR spectra of (16)	61
<b>Figure 33:</b> <sup>1</sup> H and <sup>13</sup> C NMR spectra of (17)	62
<b>Figure 35:</b> <sup>1</sup> H and <sup>13</sup> C NMR spectra of (8)	63
<b>Figure 36:</b> <sup>1</sup> H spectra of 20-(11, 11'-disulfanediyldiundecan) – camptothecin Derivative coated Gold Nanoparticles	64

## LIST OF ABBREVIATIONS

<b>CPT</b>	: 20-( <i>S</i> ) - Camptothecin
<b>TOPO-I</b>	: Topoisomerase I Enzyme
<b>SAR</b>	: Structure-Activity Relationships
<b>FDA</b>	: The US Food And Drug Administration
<b>MRI</b>	: Magnetic Resonance Imaging
<b>SUV</b>	: Small Unilamellar Vesicles
<b>LUV</b>	: Large Unilamellar Vesicles
<b>MLV</b>	: Multilamellar Vesicles
<b>PEG</b>	: Polyethylene Glycol
<b>AuNPs</b>	: Gold Nanoparticles
<b>DMAP</b>	: 4-Dimethylaminopyridine
<b>TLC</b>	: Thin Layer Chromatography
<b>DCM</b>	: Dichloromethane
<b>NMR:</b>	: Nuclear Magnetic Resonans
<b>AIBN</b>	: Azobisisobutyronitrile
<b>DMSO</b>	: Dimethylsulfoxide
<b>TEM</b>	: Tranmission Electron Microscopy

## **CHAPTER 1**

### **INTRODUCTION**

#### **1.1 Cancer**

Cancer is a disease characterized by irregular division of cells, combined with the malignant behavior of these cells. Malignant cancer cells tend to spread, either by direct growth into adjacent tissue through invasion, or by implantation into distant sites by metastasis. Ten or more years often pass between exposure to external factors and detectable cancer. Cancer may affect people at all ages, but risk tends to increase with age. It is one of the principal causes of death in developed countries.

There are many theories about the cause of cancer. At least six important factors contribute to cancer pathogenesis, including failure of apoptosis, overactivation of oncogenes, inactivation of tumor suppressor genes, cell cycle activation of quiescent cell, acquisition of metastatic behaviour by malignant cells, disordered responses to cellular growth factors, and immune system surveillance failure. New aspect of genetics of cancer pathogenesis, such as DNA methylation, and microRNAs are increasingly being recognized as important components.

Environmental stimuli, or carcinogens such as tobacco smoke, radiation, chemicals, or infectious agents, can cause cancer. The interaction between carcinogens and the host genome, to explain why some patients get cancer after exposure to a known carcinogen while others don't, is the subject of immense recent research [1].

Cancer is usually classified according to the tissue of origin more than the location of manifestations. Prognosis in most cases depends on the original staging of the disease, though increasing use of molecular markers is leading to individually tailored treatments. A definitive diagnosis usually requires the histologic

examination of a tissue biopsy specimen by pathologist, though the initial indication of malignancy can be symptoms or radiographic imaging abnormalities. Most cancers can be treated and some cured, depending on the specific type, location, and stage. Once diagnosed, cancer is usually treated with a combination of surgery, chemotherapy and radiotherapy. As research develops, treatments are becoming more specific for the type of cancer pathology. Drugs that target specific cancer cell markers, thereby minimizing damage to normal tissue, already exist for several types of malignancies [2].

## 1.2. Camptothecin

Camptothecins **1** are a class of anticancer agents that are a prototypical DNA topoisomerase I (topo I) inhibitors and appear to be active in human cancers previously resistant to chemotherapy [3].

The isolation and structure determination of 20-(*S*)- camptothecin (CPT) (**1**) (figure 1), a pentacyclic alkaloid derived from the Asian tree *Camptothica acuminata*, was first accomplished by Wall et al. in 1958.[4]

The US National Cancer Institute screening programme identified camptothecin as a drug with potential antitumour activity in 1966 [5]. It shows anticancer activity mainly against colon and pancreatic cancer cells. But its analogues showed anticancer activity in breast, liver, prostate, etc.

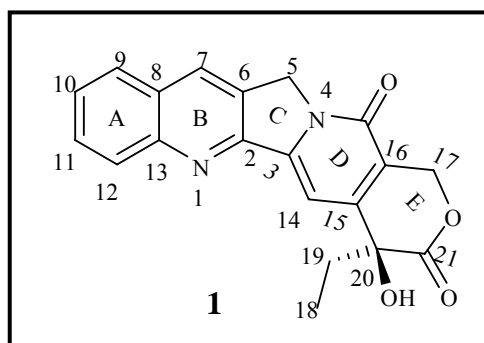


**Figure 1.** Structure of Camptothecin

The planar pentacyclic ring structure (rings A–E) (Figure 1) was suggested to be one of the most important structural features. Earlier, it was reported that the complete pentacyclic ring system is essential for its activity, but recently reported results show that the E-ring lactone is essential for its activity. This ring in the present lactone form with specific C-20 configuration is required for better activity. A brief description of its structure-activity relationships (SAR) is as follows [19]:

- Rings A–D are essential for in vitro and in vivo activity.
- Saturation of ring B: compounds show little activity.
- $\alpha$ -hydroxy lactone ring is necessary for activity.
- Oxygen at 20 is essential for activity. Replacement of this oxygen with sulfur or nitrogen abolishes the activity of CPT.
- Conformation at C-20 is crucial for better activity the 20(S) isomer is 10- to 100-fold more active than 20(R).
- D-ring pyridone is required for antitumour activity.
- Modifications in rings A and B are well tolerated and resulted in better activity than CPT in many cases.

In human clinical studies, held in the late 1960s, disappointing results were reported. Therapeutic application of unmodified CPT is hindered by very low solubility in aqueous media, high toxicity, and rapid inactivation through lactone ring **1** hydrolysis at physiological pH. Lactone hydrolysis, which is reversible in acidic media, leads to a water-soluble carboxylate **2** (Figure 2) [6]. The latter is inactive and readily binds to human serum albumin, making it inaccessible for cellular uptake [7]. More unfortunately, the sodium salt **2** is cleared by the kidneys and causes hemorrhagic cystitis and myelotoxicity, which resulted in suspension of the trials [8, 9].

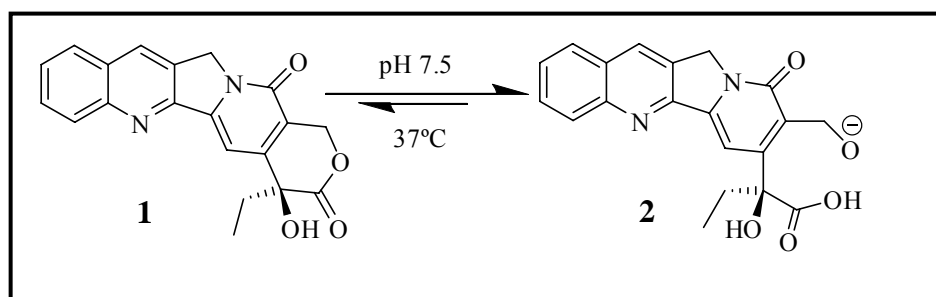


**Figure 2.** Camptothecin hydrolysis to water soluble sodium salt

An intact lactone group is essential for interaction with the DNA–enzyme complex; all camptothecin derivatives presently in clinical trials possess an E-ring lactone. This lactone moiety is chemically unstable and undergoes reversible hydrolysis to a hydroxyl carboxylate form, which is devoid of topoisomerase I inhibitory activity [10, 11, 12, 13]. The hydrolysis rate is dependent on several factors including pH [14], ionic strength [15] and protein concentration [15, 16]. Under acidic conditions (pH<4) the lactone structure predominates, whereas at pH values > 10 the open-ring form is exclusively present [15, 18]. At physiological pH, equilibrium processes favor conversion to the carboxylate form for all camptothecins except for SN- 38 . Both the lactone / carboxylate ratio at equilibrium and the rate of conversion between the two forms is affected by the pH [18]. Increased temperature increases the rate of interconversion, without affecting the equilibrium itself [17].

CPT as itself could not be used as a drug of choice due to its severe toxicity. Thus, the development of these semisynthetic strategies have facilitated the study of the CPT mechanism, as well as the identification of analogues with improved properties, including lactone stabilization, solubility and drug transport mechanisms, tumor cell recognition and enhancement of DNA sequence specificity. These above structural models provide insight regarding the mechanism of action of CPT, and understanding of how systematic modifications within the CPT structure may enhance or suppress the effect of the drug in a biological context.

In view of the clinical success of the water-soluble CPT derivatives topotecan (Hycamtin) (**3**) (Figure 3) and irinotecan (Camptosar) (**4**) (Figure 4), which effort to increase the water solubility of camptothecin have comprised a major research focus [20, 21].

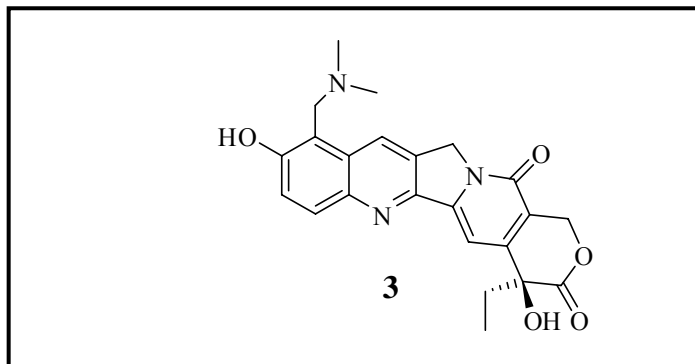


**Figure 3.** Structure of topotecan

Topotecan (9-[(dimethylamino) methyl]-10-hydroxycamptothecin) (**3**) (Figure 3) was the first camptothecin analogue to be approved for clinical use by the US Food and Drug Administration (FDA). It is water-soluble because of its side-chain at carbon 9 of the A ring. Results of preclinical studies suggested topotecan to have excellent antitumour activity in vitro [22]. Tumour xenograft models showed activity in many tumour types, including adenocarcinomas of the ovary and colon, tumours of the central nervous system, and sarcomas [23, 24] .

Irinotecan (7-ethyl-10-[4-(1-piperidino)-1-piperidino] carbonyloxy camptothecin) (**4**) (Figure 4) was the first water-soluble semisynthetic derivative of camptothecin to enter clinical trials. A unique characteristic of irinotecan is its bulky dipiperidino sidechain linked to the camptothecin molecule via a carboxyl-ester bond. This side-chain, although providing necessary solubility, leads to a substantial reduction in anticancer activity. Cleavage of the side-chain by rboxylesterases — found mainly in the liver and gastrointestinal tract — forms the metabolite SN-38, **5**, (7-ethyl-10-hydroxycamptothecin). Irinotecan became commercially available in Japan in 1994,

where its approved indications were cancers of the lung (small-cell and non-small-cell), cervix, and ovaries. It was approved in Europe in 1995 as a second-line agent for colon cancer, 1 year before European approval of topotecan. Irinotecan was approved in the USA in 1996 for treatment of advanced colorectal cancer refractory to fluorouracil. Additional CPT analogues are also under investigation, and are also of interest in combination regimens as radiation sensitizers. [25]

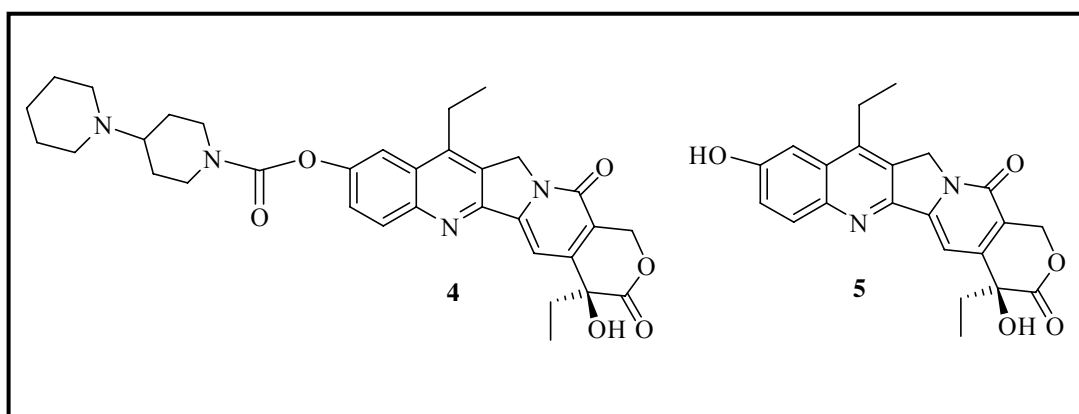


**Figure 4.** Structure of Irinotecan and SN38

### 1.2.1 DNA Topoisomerases

The majority of clinically approved anticancer agents are small molecules which damage DNA either directly through cleavage (e.g. bleomycin) or alkylation (e.g. cisplatinum) reactions, or indirectly through inhibition of nucleic acid precursor biosynthesis or inhibition of enzymes which modulate DNA topology, such as the topoisomerases [26].

Topoisomerases are essential nuclear enzymes that modify the topological state of DNA through the introduction of transient breaks in the phosphodiester backbone of DNA [27, 28]. They can relax torsional stress in supercoiled DNAs and resolve topologically complex DNA molecules via unknotting and decatenation. The topoisomerases have essential roles in the key cellular processes of replication and

transcription [29, 30]. This is the basic reaction catalyzed by the topoisomerases. Initially, topoisomerases were simply classified as either type I or type II enzyme depending on whether they catalyzed their reactions by making transient single strand DNA breaks (the type I enzyme) or transient double strand DNA breaks (the type II enzyme). Human DNA topoisomerases are the archetype of mammalian DNA topoisomerases. Human Topo I is a monomeric protein, encoded by a single-copy gene located on human chromosome 20q12–13.2. Human Topoisomerase II on the other hand, is a homodimeric protein, encoded by a single copy gene on human chromosome 17q21-22[31].

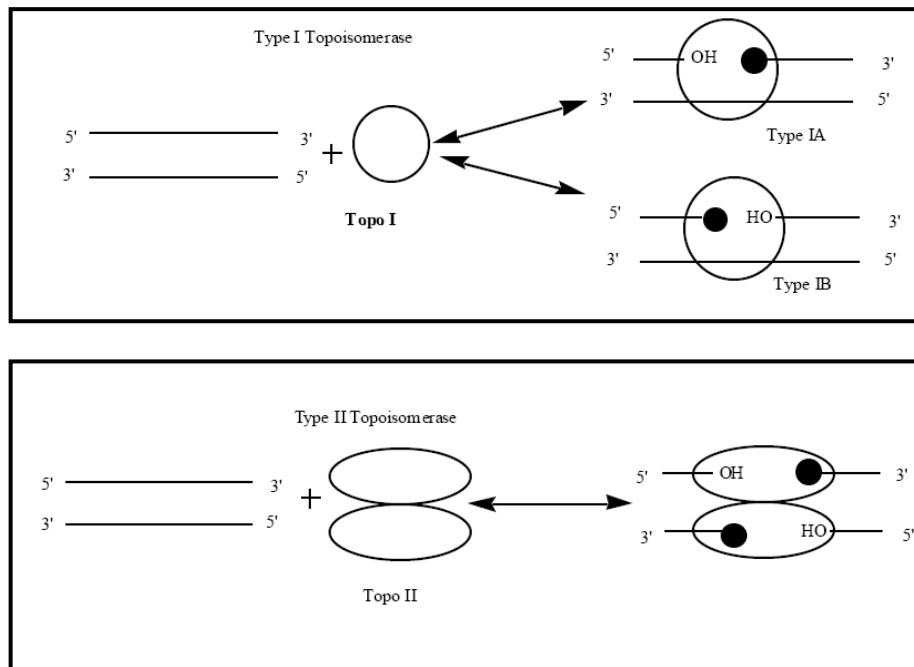


**Figure 5:** Mechanism of Relaxation DNA by Topoisomerase I and Topoisomerase II

This mechanistic description is still correct but has become slightly more complicated with the recent discovery of new members of the topoisomerase family [32]. The type I enzymes have been further divided in two distinct subgroups with no sequence similarity, Type I A (including prokaryotic type I topoisomerases) and

type I B (including eukaryotic type I topoisomerases) (Figure 5). Type I A enzymes require magnesium as a cofactor and attack a single-stranded stretch of DNA to produce a transient covalent complex where the enzyme is attached to the 5'-end of the nicked single strand and relax only negatively. On the contrary, topoisomerase I B requires no metal ions or single-stranded region for function to form a transient DNA-(3'-phospho-tyrosyl) - enzyme intermediate and is able to relax both positive and negative supercoils [33].

Topo II relaxation of DNA requires ATP and results in a change in linking number by (multiples of) two. In contrast, the mechanism of DNA relaxation by topo I involves the transient single strand cleavage of duplex DNA, unwinding and religation. Specifically, topo I mediated DNA strand scission involves a nucleophilic attack on phosphodiester backbone by the 5'-OH DNA (reverse) or tyrosine (forward) nucleophile is greatly activated by specific contacts between the non bridging scissile phosphodiester oxygens and the side chains of two arginines (Arg<sup>488</sup> and Arg<sup>590</sup>), a lysine (Lys<sup>532</sup>) and a histidine (His<sup>632</sup>) residues. These interactions would facilitate the formation of a pentacoordinate phosphorane transition state. The His<sup>632</sup> residue would serve to stabilize this pentavalent transition state through hydrogen bonding to one of the nonbridging oxygens, as depicted in. In the reverse reaction, the attack to the phospho-tyrosine linkage by the 5' -OH DNA expels the active site tyrosine residue of the enzyme; the resulting intermediate is termed the 'covalent binary complex'. (Figure 6) [34].

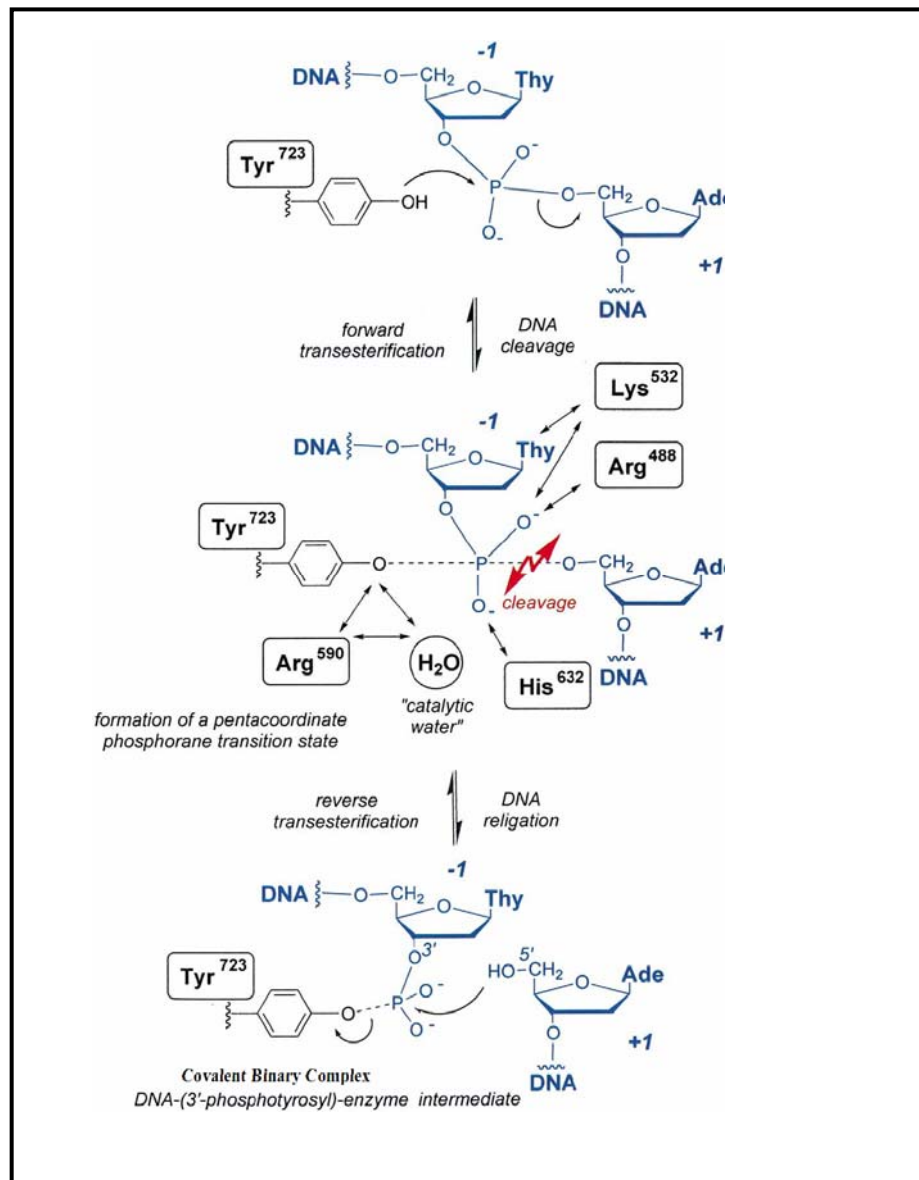


**Figure 6:** Mechanism of DNA relaxation by topoisomerase I

Following DNA relaxation via passage of the broken DNA strand around the unbroken strand, the phosphodiester backbone is reformed by religation with concomitant release of the enzyme. Inhibitors of both topo I and topo II are characterized by their ability to stabilize the covalent binary complex, thus diminishing religation and ultimately DNA synthesis and cell viability [31].

### **1.2.2 Camptothecins as Topoisomerase Poisons: Mechanism of Action**

Numerous topo I inhibitors have been characterized, including rebeccamycin, indolocarbazole, nitidine and 2-phenylbenzimidazole [35]. The CPT family, however, remains the most extensively studied class of agents that target topo I.

CPTs act by binding to the topoisomerase I-DNA complex, leading to an accumulation of DNA strand breaks upon replication, ultimately causing cell death during the S-phase of the cell cycle. The complex is normally a transient intermediate involved in DNA relaxation during a number of critical cellular processes, including replication, transcription, recombination, repair, chromatin assembly, and chromosome segregation, and generally rapidly reversible without CPT [36,37].

Overwhelming evidence has supported the view that cell killing by camptothecin is due to the formation of topoisomerase I-camptothecin-DNA cleavable complexes [38, 39]. Inhibition of relaxation activity of topoisomerase I is apparently inconsequential as far as cell killing concerned. [38].

Studies with replication inhibitors have shown that transient inhibition of DNA replication during camptothecin treatment can completely abolish camptothecin cytotoxicity, suggesting an involvement of active DNA replication in camptothecin [40, 41, 42]. Studies in a cell-free SV-40 replication system have further suggested a fork collision model for camptothecin cytotoxicity [40]. In this model, the interaction between the replication fork and the topoisomerase I-camptothecin-DNA cleavable complex is presumed to be the lethal event and results in at least three detectable changes: irreversible arrest of DNA replication forks, double-strand DNA breaks at the forks, and the conversion of reversible cleavable complexes into cleaved complexes (Figure 7). Presumably one of these several changes is trigger for cell death and G2 cell cycle arrest [40, 43].

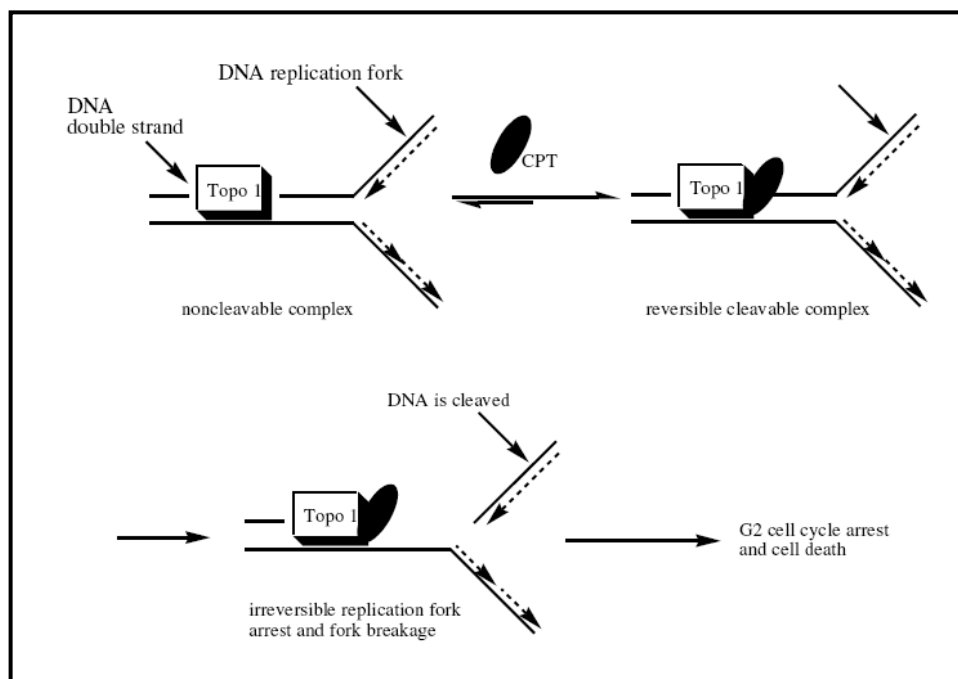


**Figure 7:** Mechanism of action of Camptothecin

### 1.2.3 Structural Models for the Ternary Cleavable Complex Formed Between Human Topo I, DNA, and CPT

Several structural models have been suggested for the interaction of CPT with the covalent binary complex. The X-ray crystal structure of the human topoisomerase I-DNA cleavable complex was used to identify the general models for the ternary drug-DNA-Topo I cleavable complex formed with camptothecin and its analogs [51].

The Hol group firstly reported a crystal structure of the binary human topo I-DNA cleavable complex [44]. The crystal structure affords the convenience of model studies of the ternary drug-DNA-Topo I via computer techniques. The Hol group proposed a model for the ternary cleavable complex in which the +1 guanine flips out of the DNA helix and stacks with the CPT molecule (Figure 8).

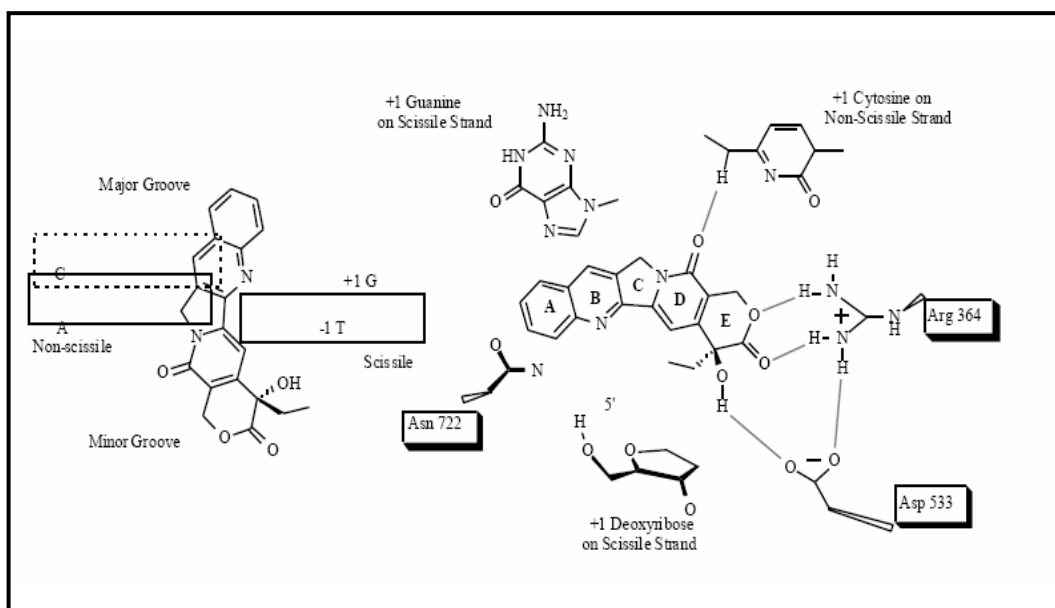


**Figure 8:** Hol Base- Flipping Model

In Pommier's proposed drug-stacking model, he argued that CPT was pseudointercalated in the topo I-DNA cleavable site and interacted with the protein near its catalytic tyrosine *via* stacking and hydrogen bonding to specific amino acid and DNA residues (Figure 9) [45].

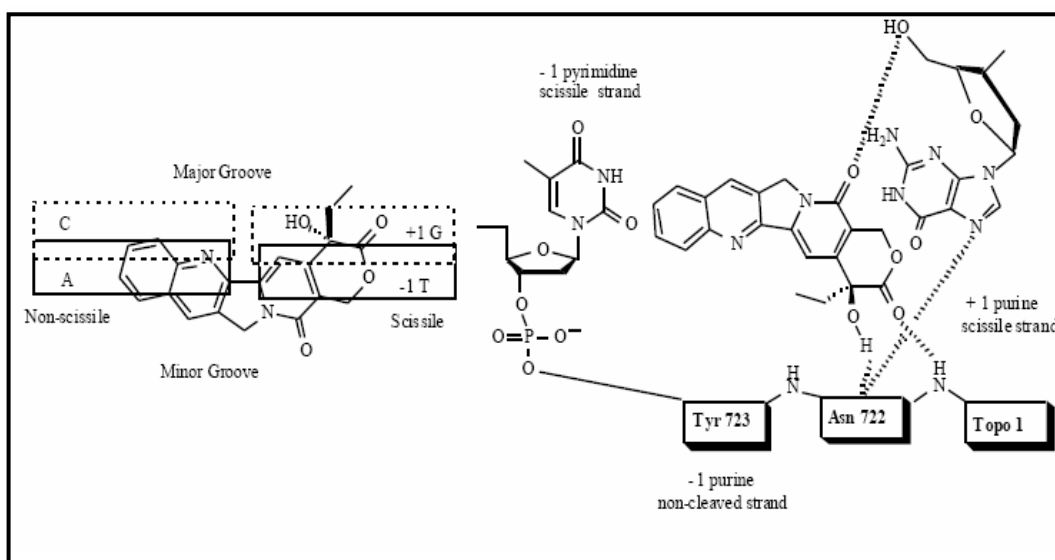


**Figure 9:** Pommier Intercalation Model

The recent binding models were greatly facilitated by X-ray crystal structures of topo I interacting both covalently and noncovalently with DNA [46]. Kerrigan et al. derived a ternary 20(*S*)-CPT-DNA-TOP1 cleavable complex structure suggesting that Arg364, Asp533, and Asn722 are the closest amino acid residues to the intercalated drug (Figure 10).

Arg364 and Asp533 lie in the DNA minor groove, while Asn722 lies on the major groove side of the cleavage site. These amino acid residues, as well as the -1 and +1 base pairs of the DNA, represent the potential sources for favorable interactions with the bound drug. The hydrogen bonding interactions (using a distance cutoff of 3.1 Å) of 20(*S*)-CPT with both the DNA and topo1 are also schematically presented in Figure 9.

Inspection of this figure reveals that 20(*S*)-CPT stabilizes the cleavable complex primarily through hydrogen bonding interactions involving its E- and B-rings. Specifically, both the O atom and the 21-carbonyl oxygen of the E-ring make multiple hydrogen bonding contacts with Arg364. In addition, the 20-hydroxyl proton is capable of making a hydrogen bond with either the N3 atom of the +1 guanine or DNA furanose ring oxygen. The N1 atom on the B-ring of 20(*S*)-CPT makes hydrogen bonding contacts to both the 3NH proton of the -1 thymine as well as the 6-NH<sub>2</sub> group of the adenine complement to the -1 thymine. In addition to these hydrogen bonding interactions, stacking interactions between the C-ring of the drug and the adenine complement to the -1 thymine also contribute to the stability of the ternary cleavable complex. In the aggregate, these observations suggest that 20(*S*)-CPT stabilizes the TOPO1-DNA cleavable complex through an array of van der Waals and hydrogen bonding interactions with both the enzyme and the DNA [47].



devices by manipulating and working with atoms and molecules down on the scale. The “nano” in nanotechnology means one billionth that is about 10,000 times smaller than the diameter of a human hair.

American physicist and Nobel Prize winner, Richard Feynman is accounted as the inspirational father of nanotechnology for introducing the idea of molecular manufacturing, in a lecture, “There is Plenty of Room at the Bottom” [48] in 1959. However, the origins of nanotechnology did not occur until then. He attracted his audience’s attention by suggesting that what if one could build materials and devices with manipulating and controlling them at the molecular level.

In 1974, Norio Taniguchi introduced the term “nanotechnology” to represent extra-high precision and ultra-fine dimensions, and also predicted improvements in integrated circuits, optoelectronic devices, mechanical devices, and computer memory devices.

This is the so-called ‘top-down approach’ of carving small things from large structures. In 1986, K. Eric Drexler in his book “Engines of Creation” discussed the future of nanotechnology, particularly the creation of larger objects from their atomic and molecular components, the so-called “bottom-up approach”. He proposed ideas for “molecular nanotechnology”, which is to produce any kind of object from elemental particles [49].

Nanotechnology is intuitive since everything in nature is built upward from the atomic level to define limits and structures to everything. Understanding and developing nanotechnology, therefore, depends on understanding these limits and how far they can be pushed. Nanomedicine or the development of effective clinical treatments based on nanotechnology is one of the first categories of nanotechnology to bear fruit from the considerable investments being made in nanotechnology research.

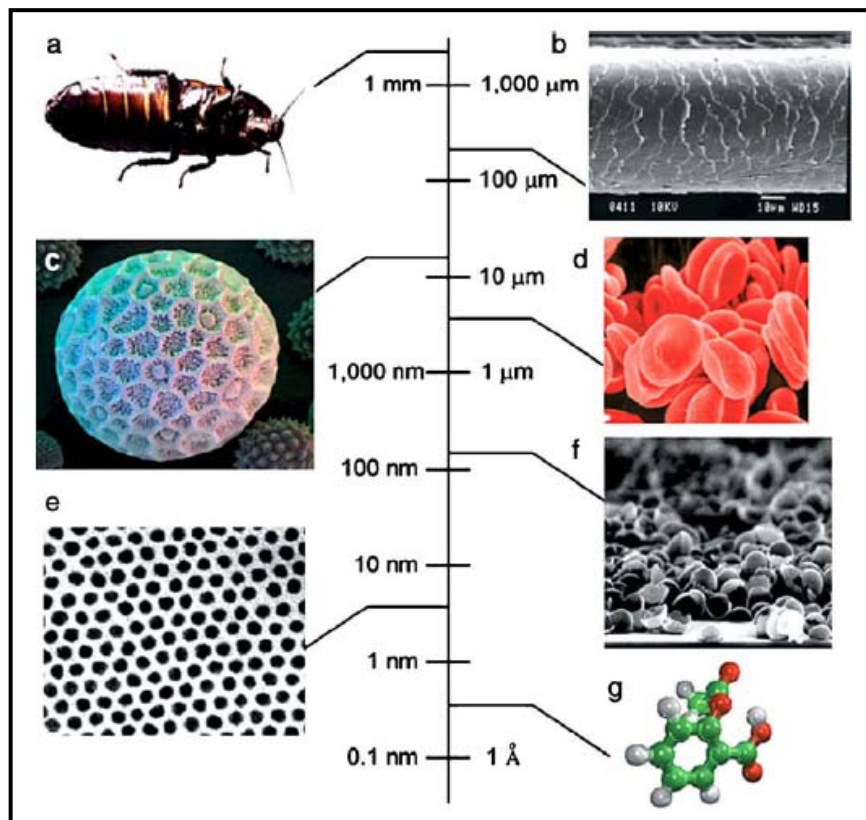


**Figure 11:** Relative sizes of small objects including (a) cockroach, (b) human hair, (c) pollen grain, (d) red blood cells, (e) aggregates of half shells of palladium, (f) superlattice of cobalt nanocrystals, and (g) aspirin molecule.

Nanomedicine depends on several overlapping molecular technologies, which are themselves subsumed within young, but progressively developing fields including (a) the construction of nanoscale-sized structures for diagnostics, biosensors, and local drug delivery; (b) the ongoing revolution in genomics, proteomics, and nano-engineered microbes; (c) the creation of molecular machines capable of identifying and eliminating host pathogens, replacing/repairing cells or cellular components in vivo.

### 1.3.1. Nanomedicine

Many approaches to nanomedicine being pursued today are already close enough to fruition that it is fair to say that their successful development is almost inevitable,

and their subsequent incorporation into valuable medical diagnostics or clinical therapeutics is highly likely and may occur very soon.

#### **1.3.1.1. Immunoisolation**

One of the simplest medical nanomaterials is a surface perforated with holes, or nanopores. In 1997, Desai et al created what could be considered as one of the earliest therapeutically helpful nanomedical devices, using bulk micromachining to fabricate tiny chambers within single crystalline silicon wafers in which biologic cells can be placed [50]. The chambers interface with the surrounding biologic environment through polycrystalline silicon filter membranes micromachined to present a high density of uniform nanopores as small as 20 nm in diameter. These pores are large enough to allow small molecules such as oxygen, glucose, and insulin to pass but are small enough to impede the passage of much larger immune system molecules such as immunoglobulins and graft-borne virus particles.

Microcapsules containing easily harvested replacement pig islet cells could be implanted beneath the skin of some diabetes patients, temporarily restoring the body's glucose control feedback loop, while avoiding the use of powerful immunosuppressants that can leave the patient at serious risk for infection. Supplying encapsulated new cells to the body could also be a valuable way to treat other enzyme- or hormone-deficiency diseases, including encapsulated neurons that could be implanted in the brain and then be electrically stimulated to release neurotransmitters, possibly as part of a future treatment for Alzheimer's or Parkinson's diseases[51].

#### **1.3.1.2. Gated nanosieves**

The flow of materials through nanopores can be externally regulated [52]. The first artificial voltage-gated molecular nanosieve was fabricated by Nishizawa et al at Colorado State University in 1995; it had an array of cylindric gold nanotubules with inside diameters as small as 1.6 nm [53]. When tubules were positively charged, positive ions were excluded and only negatively charged ions were

transported through the membrane; with a negative voltage, only positively charged ions could pass. Similar nanodevices are now combining voltage gating with pore size, shape, and charge constraints to achieve precise control of ion transport with significant molecular specificity [54]. Martin and Kohli's recent efforts have been directed at immobilizing biochemical molecular recognition agents such as enzymes, antibodies, and other proteins, and DNA, inside the nanotubes to make active biologic nanosensors and also to perform drug separations or to allow selected biocatalysis[55, 56, 57].

### **1.3.1.3. Superparamagnetic nanoparticles**

Superparamagnetic nanoparticles refer to iron oxide particles or magnetite ( $\text{Fe}_3\text{O}_4$ ) particles that are less than 10 nm in diameter. They have been around for years as contrasting agents for magnetic resonance imaging (MRI). As with other nanoparticles, functionalization of these superparamagnetic nanoparticles is getting functionalized so as to permit specific tumor targeting.

Iron oxide nanoparticles can be water-solubilized with hydrophilic polymer coatings, such as dextran or PEG. In fact, attaching PEG to nanoparticles in general, not just to iron oxide particles, is a well documented means of sterically preventing opsonization of nanoparticles in the serum and reducing their uptake by the reticuloendothelial system. This effectively enhances biocompatibility and increases the circulation time of nanoparticles [58]. Iron oxide nanoparticles can also be made hydrophobic by coating with aliphatic surfactants or liposomes (resulting in magnetoliposomes) [59].

Magnetic nanoparticles can be remotely activated using electromagnetic fields, and they can also be used to treat cancers thermally [60]. Under the influence of an alternating field, superparamagnetic nanoparticles undergo relaxation, in which heat is generated by the rotation of particles in the field. Most recently, superparamagnetic nanoparticles have been used in clinical thermotherapy of locally recurrent prostate cancer [61]. Thermotherapy is defined as the ability to attain at least hyperthermic temperatures of up to  $42^\circ\text{C}$ , which can render cancer

cells more susceptible to the effects of radiation and cause some apoptosis [61]. Because of the very low clearance rate of these nanoparticles from the tumor mass, serial thermotherapy treatments can follow a single magnetic fluid injection, and the patients received six thermotherapy treatments of 60 minutes duration at weekly intervals.

#### **1.3.1.4. Ultrafast DNA Sequencing**

Branton et al use an electric field to drive a variety of RNA and DNA polymers through the central nanopore of an  $\alpha$ -hemolysin protein channel mounted in a lipid bilayer similar to the outer membrane of a living cell [62, 63]. Branton first showed that the nanopore could rapidly discriminate between pyrimidine and purine segments along a single RNA molecule and then in 2000 demonstrated discrimination between DNA chains of similar length and composition differing only in base pair sequence. Reliability and resolution are the biggest challenges and researches continue to perfect this approach [64-68]. Current research is directed toward fabricating pores with specific diameters and repeatable geometries at high precision [69-72], understanding the unzipping of double-stranded DNA as one strand is pulled through the pore [73] and the recognition of folded DNA molecules passing through a pore, and investigating the benefits of adding electrically conducting electrodes to pores to improve longitudinal resolution "possibly to the single-base level for DNA" [68]. If these difficult challenges can be surmounted, nanopore-based DNA-sequencing devices could allow per pore read rates potentially up to 1000 bases per second [74].

#### **1.3.1.5. Fullerene-Based Pharmaceuticals**

Soluble derivatives of fullerenes such as C<sub>60</sub>—a soccerball– shaped arrangement of 60 carbon atoms per molecule— show great promise as pharmaceutical agents. These derivatives, many already in clinical trials, have good biocompatibility and low toxicity even at relatively high dosages. Fullerene compounds may serve as antiviral agents (most notably against human immunodeficiency virus [75]), antibacterial agents (Escherichia coli [76], Streptococcus [77], Mycobacterium

tuberculosis [78]), photodynamic antitumor [79, 80] and anticancer [81] therapies, antioxidants and antiapoptosis agents as treatments for amyotrophic lateral sclerosis [82] and Parkinson's disease, and other applications.

### **1.3.1.6. Liposomes**

The first suggested use of liposomes came from the group of Weismann in 1969 [83]. Since then liposomes have been used as a versatile tool in biology, biochemistry and medicine [84]. Liposomes are small artificial vesicles of spherical shape that can be produced from natural non-toxic phospholipids and cholesterol. Because of their size, hydrophobic and hydrophilic character, as well as biocompatibility, liposomes are promising systems for drug delivery. Liposome properties vary substantially with lipid composition, size, surface charge and the method of preparation. They are therefore classified into three classes based on their size and number of bilayers. Small unilamellar vesicles (SUV) are surrounded by a single lipid layer and are 25–50 nm in diameter. Large unilamellar vesicles (LUV) are a heterogeneous group of vesicles similar to SUVs and are surrounded by a single lipid layer. Multilamellar vesicles (MLV), however, consist of several lipid layers separated from one another by a layer of aqueous solution.

Drugs associated with liposomes have markedly altered pharmacokinetic properties compared to drugs in solution. They are also effective in reducing systemic toxicity and preventing early egradation of the encapsulated drug after introduction to the target organism [85, 86]. Liposome surfaces can be readily modified by attaching polyethylene glycol (PEG)-units to the bilayer (producing what is known as stealth liposomes) to enhance their circulation time in the bloodstream [87]. Furthermore, liposomes can be conjugated to antibodies or ligands to enhance target-specific drug therapy.

### **1.3.1.7. Nanoshells**

Halas and West at Rice University in Houston have developed a platform for nanoscale drug delivery called the nanoshell—dielectric metal (gold-coated silica)

nanospheres whose optical resonance is a function of the relative size of the constituent layers [88]. These nanoshells, embedded in a drug-containing tumor-targeted hydrogel polymer, and then injected into the body, accumulate near tumor cells. When heated with an infrared laser, the nanoshells (each slightly larger than a polio virus) selectively absorb a specific infrared frequency, melting the polymer and releasing the drug payload at a specific site. Nanoshells might prove useful in treating diabetes—a patient would use a ballpointpen sized infrared laser to heat the skin site where nanoshell polymer had been injected, releasing a pulse of insulin. Unlike injections, which are taken several times a day, the nanoshell-polymer system could remain in the body for months [89].

#### **1.3.1.8. Dendrimers**

Dendrimers, a unique class of polymers, are highly branched macromolecules whose size and shape can be precisely controlled [90, 91]. Dendrimers are fabricated from monomers using either convergent or divergent step growth polymerization. The welldefined structure, monodispersity of size, surface functionalization capability, and stability are properties of dendrimers that make them attractive drug carrier candidates. Drug molecules can be incorporated into dendrimers via either complexation or encapsulation. Dendrimers are being investigated for both drug and gene delivery [92, 93], as carriers for penicillin [91], and for use in anticancer therapy [94, 95]. Dendrimers used in drug delivery studies typically incorporate one or more of the following polymers: polyamidoamine [96, 97], melamine [98], poly (L-glutamic acid) [99], polyethyleneimine [99], poly (propyleneimine) [100], and poly (ethylene glycol) [100], Chitin and chitosan have also been incorporated with dendrimers [101].

#### **1.3.1.9. Metal structures**

Hollow metal nanoshells are being investigated for drug delivery applications [102]. Typical fabrication methods involve templating of the thin metal shell around a core material such as a silica nanoparticle. Typical metals include gold, silver, platinum, and palladium. When linked to or embedded within polymeric drug carriers, metal

nanoparticles can be used as thermal release triggers when irradiated with infrared light or excited by an alternating magnetic field [103]. Biomolecular conjugation methods of metals include bifunctional linkages, lipophilic interaction, silanization, electrostatic attraction, and nanobead interactions [104].

### **1.3.2. Gold Nanoparticles**

Nanosized particles of noble metals, especially gold nanoparticles (AuNPs), have received great interests due to their attractive electronic, optical, and thermal properties as well as catalytic properties and potential applications in the fields of physics, chemistry, biology, medicine, and material science and their different interdisciplinary fields [105]. Therefore, the synthesis and characterization of AuNPs have attracted considerable attention from a fundamental and practical point of view. As is known, the preparation of AuNPs generally involves the chemical reduction of gold salt in aqueous, organic phase or two phases. However, the high surface energy of AuNPs makes them extremely reactive, and most systems undergo aggregation without protection or passivation of their surfaces. Thus, special precautions have to be taken to avoid their aggregation or precipitation. Typically, AuNPs are prepared by chemical reduction of the corresponding transition metal salts in the presence of a stabilizer which binds to their surface to impart high stability and rich linking chemistry and provide the desired charge and solubility properties. Some of the commonly used methods for surface passivation include protection by self-assembled monolayers, the most popular being citrate [106] and thiol-functionalized organics [107]; encapsulation in the H<sub>2</sub>O pools of reverse microemulsions [108]; and dispersion in polymeric matrixes [109]. Although the synthesis of AuNPs makes great progress, how to control the size, monodisperse, morphology, and surface chemistry of AuNPs is still a great challenge. Recently, designing novel protectors for AuNPs have been the focus of intense research because surface chemistry of AuNPs will play a key role in future application fields such as nanosensor, biosensor, catalysis, nanodevice and nanoelectrochemistry. Thus, in the synthesis part, we will focus on recent advances on how to choose novel protecting agents for the synthesis of AuNPs. For electroanalytical chemist, more attention has been paid to AuNPs because of their

good biological compatibility, excellent conducting capability and high surface-to-volume ratio. The introduction of AuNPs onto the electrochemical interfaces has infused new vigor into electrochemistry [110]. The development of nanomaterial will offer new opportunities in the development of electroanalytical chemistry. Recently, AuNPs modified electrode surfaces, generating functional electrochemical sensing interfaces, have been reported in great quantity.

#### **1.4. Aim of the Work**

In this study, modification of the CPT structure in order to improve its stability and solubility without reducing its activity was investigated. There are many attempts for the synthesis of new functionally improved molecules in which functionalization of CPT at 20-OH position with suitable linker. Retrosynthetic analysis of modification of CPT from 20- OH position is shown in figure 12.

Our approach consists of two main titles, modification from 20-OH position and synthesis of CPT-linker coated gold nanoparticles. Drug coated gold nanoparticles offers advantages that allow a more targeted drug delivery and a more controllable release of a therapeutic compound.

In future, all physical, chemical and biological properties of the particles will be determined. Additional study about the cleavage of the linker will be carried out to release the anticancer drugs by using ultraviolet, laser X-ray, electrochemical or enzymatic reactions.

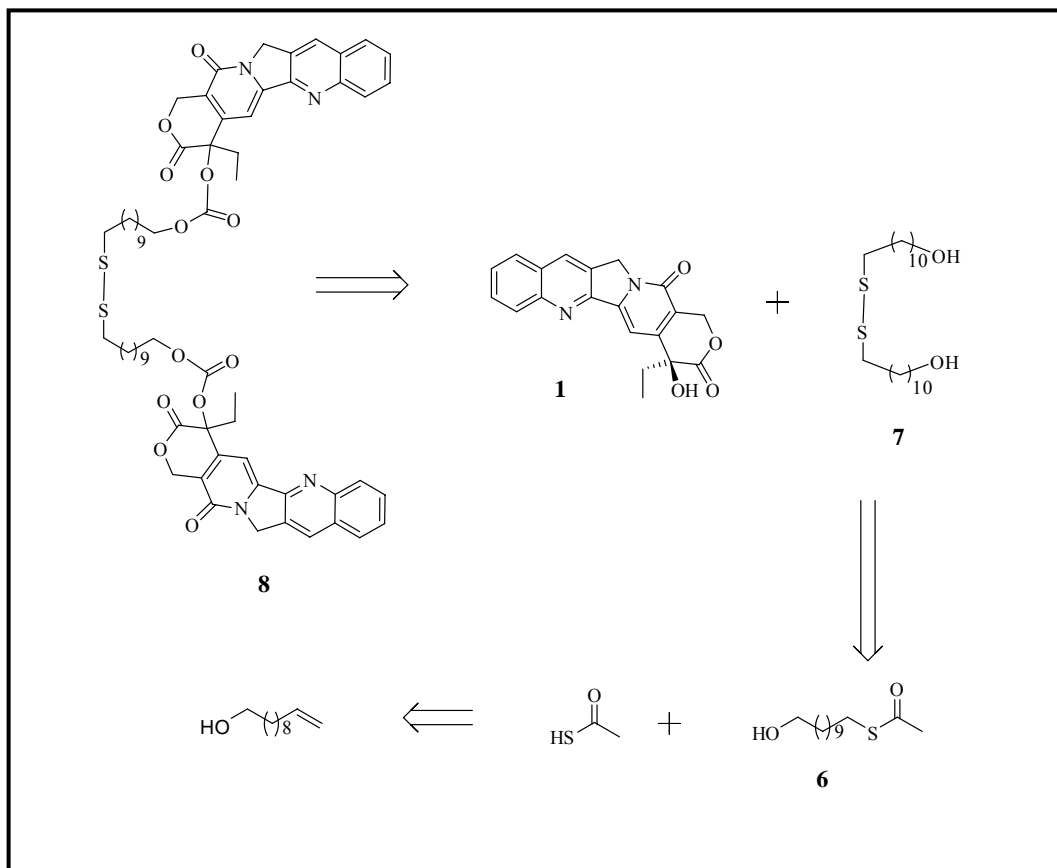


**Figure 12.** Retrosynthetic analysis of modification of CPT at 20 - OH position

## CHAPTER 2

### RESULTS & DISCUSSION

The clinical application of CPT to cancer treatment was suspended because of its unfavorable properties such as non-specific toxicity and negligible water solubility [111]. Another key problem is the structural instability of the 20-hydroxy lactone ring moiety, which is easily hydrolyzed into an inactive *E*-ring-opened carboxylate form under physiological conditions (Scheme 1) [112].

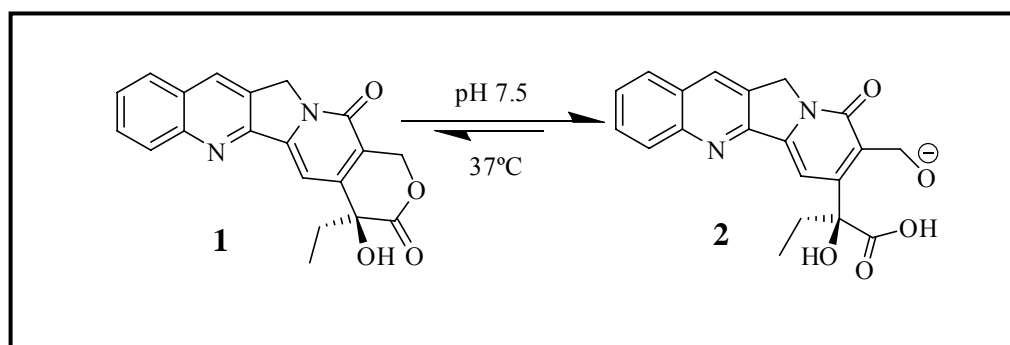


**Figure 2.** Camptothecin hydrolysis to water soluble sodium salt

#### 2.1. Modifications in E Ring

The  $\alpha$ -hydroxy lactone system of ring E has been found to be important for the inhibition of the topoisomerase enzyme as well as for in vivo potency. Modifications in E ring generally reduce or abolish the activity. Under physiological conditions, due to  $\alpha$ -hydroxy group, the lactone ring is opened to inactive carboxylate group.

Cao et. al. proposed the intact lactone ring would be better protected if camptothecins were transformed into the corresponding water-soluble alkyl esters [113]. This proposal is supported by Fassberg and Stella who have postulated that CPT lactone ring opening arising from nucleophilic attack at the acyl carbon, probably involves the 20-OH group in one of the proton-transfer steps or in stabilizing the transition state perhaps via a strong intramolecular H-bond as shown in scheme 3 [114].

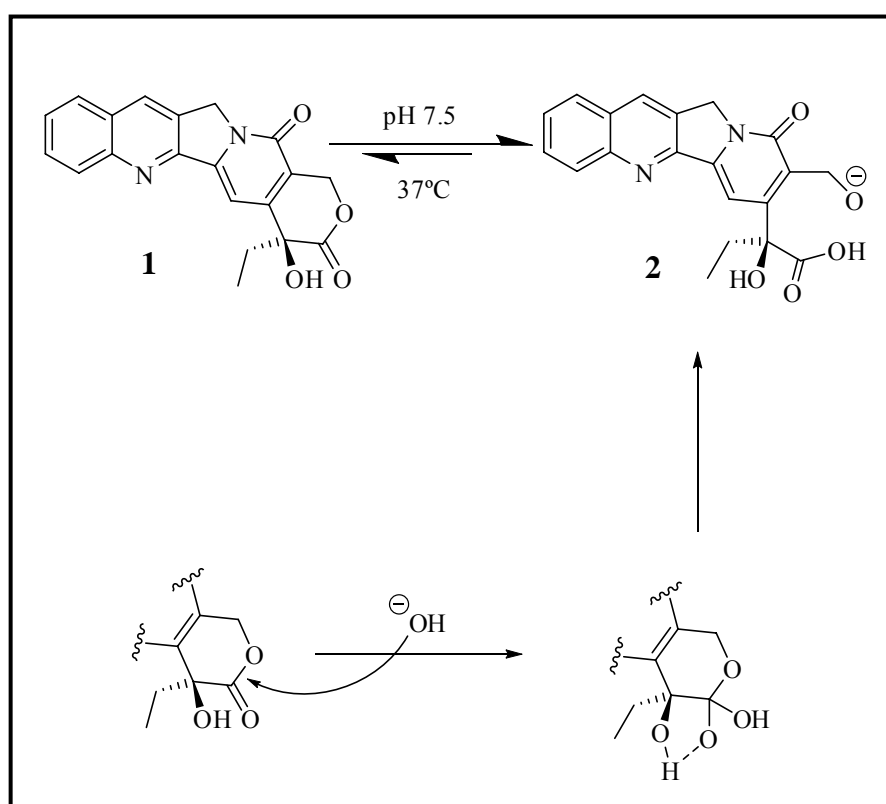


**Figure 13.** Mechanism of camptothecin hydrolysis to water soluble sodium salt

Based on this strategy, E-ring modifications have underscored the stability of lactone. Hertzberg et al. replaced the 21-C with other atom such as N and S to lactam **9** and thiolactone **10**, thereby reducing the tendency of the E-ring to open (Figure 14) [115]. However, the resulting CPT lactam **9** and thiolactone **10** were essentially inactive.

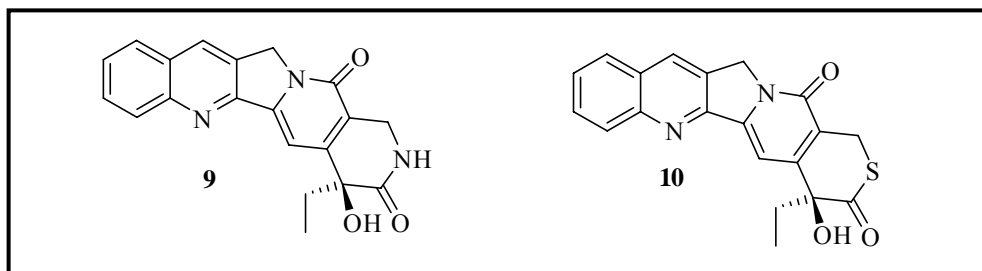


**Figure 14.** Structures of CPT lactam and thiolactone

The replacement of 20-OH group has been exploited to afford 20 - amino CPT **11**, 20-deoxyCPT **12a**, and halogenated CPTs **12b**, **12c**, which were all shown to have significantly diminished activity (Figure 15) [116].

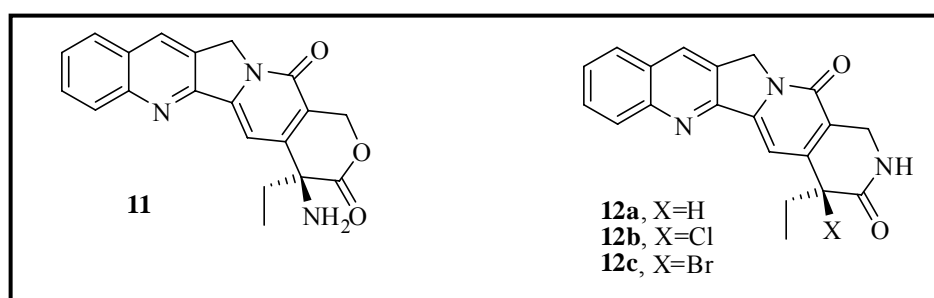


**Figure 15.** Structures of 20- aminoCPT, 20-deoxyCPT, and halogenated CPTs

Additional attention has been paid to esterification of 20 - hydroxyl group, which can either eliminate the intramolecular hydrogen bonding or increase the steric hindrance of carbonyl group of E-ring [117, 118]. Pan et al. reported some 20-O-linked nitrogen-based camptothecin ester derivatives including ester **13**, which possesses both lower cytotoxic in vitro and better antitumor activity in vitro than topotecan. Rahier prepared four 20-O-phosphate and phosphonate analogs of CPT **14a**, **14b**, **14c**, **14d** (Figure 16) [119]. While these derivatives were less potent than CPT, stabilization was improved significantly. The experimental evidence revealed that esterification of 20-OH markedly reduced the toxicity of CPT analogs.

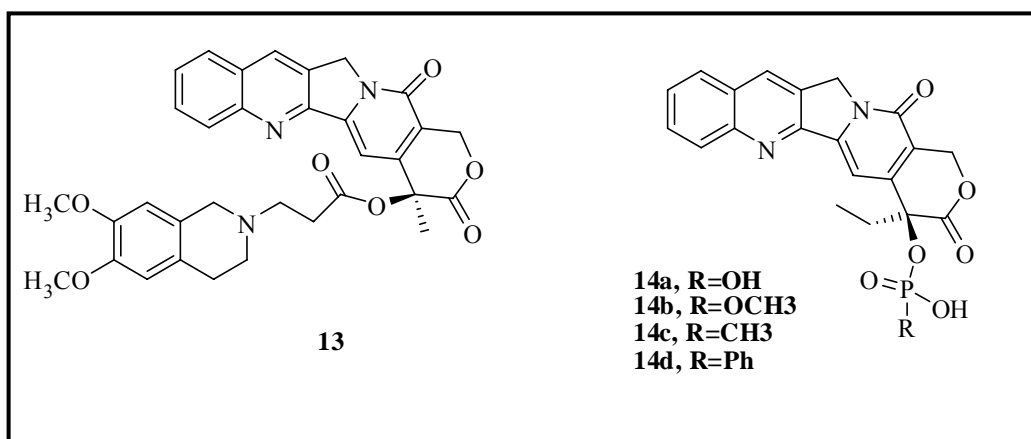


**Figure 16.** Structures of 20-O-linked nitrogen-based camptothecin ester derivatives and phosphonate analogs of CPT

In the present study, three main goals were objected to be achieved; demonstration of improved stability, improved solubility and targeted release of new camptothecin derivatives. The main objective of the study addressing these goals is the conjugation of removable protecting group to CPT from 20-OH position. The designed molecules are shown in the figure 17 below.

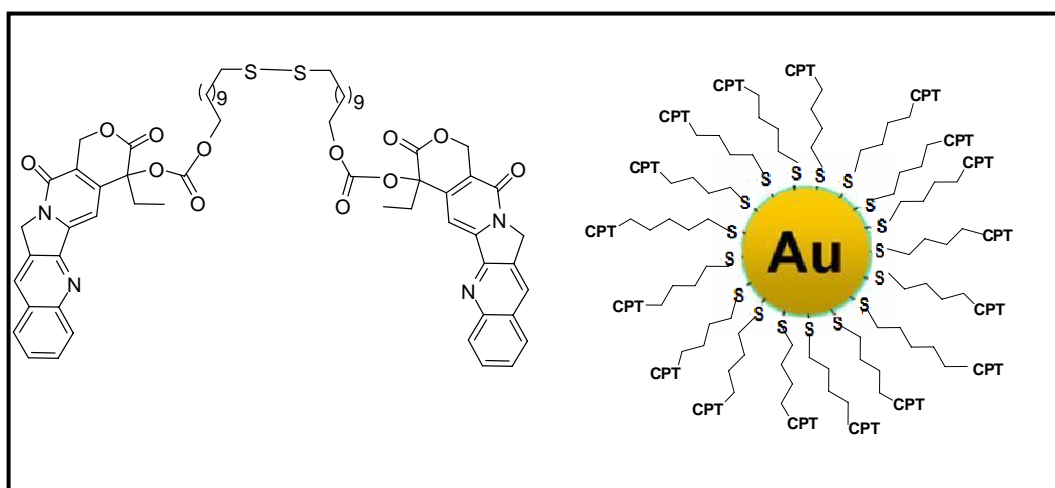
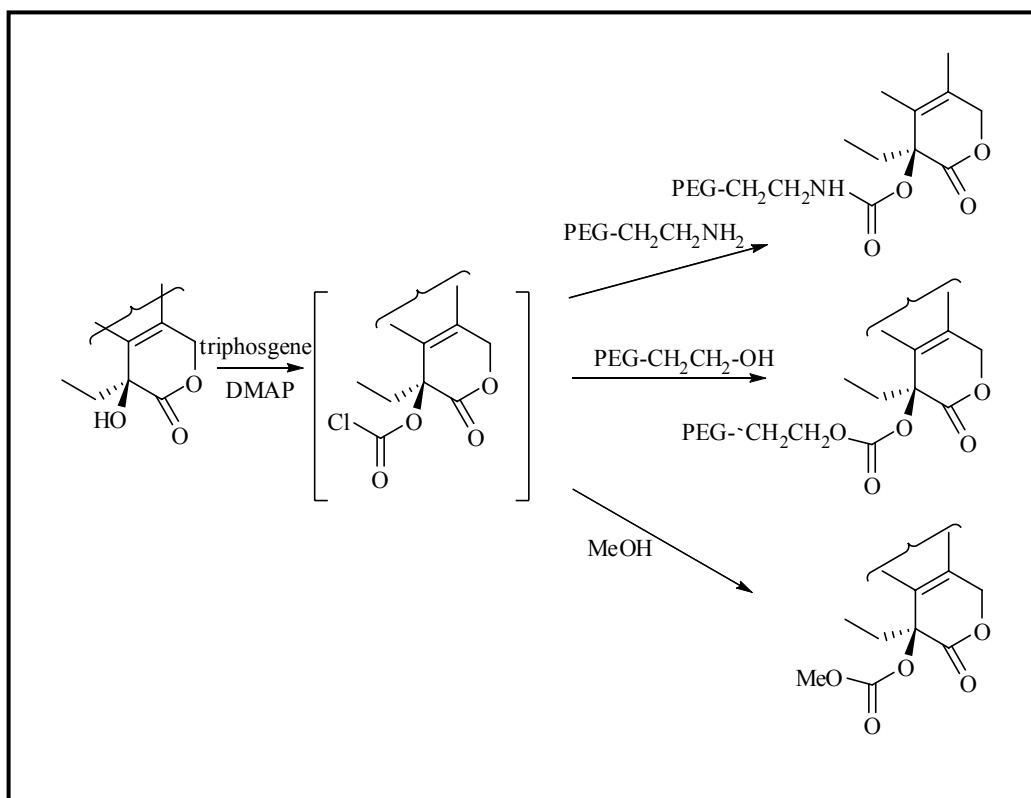


**Figure 17:** Target Molecules

## 2.2. Synthesis of 20-(11, 11'-disulfaneyldiundecan)camptothecin

As it is mentioned above the E-lactone ring of camptothecin including the 20-hydroxyl group is considered to be essential moiety for the drug's activity. Stabilization of this ring via protecting the hydroxy group was studied by many different groups and more stable camptothecin analogs were synthesized.

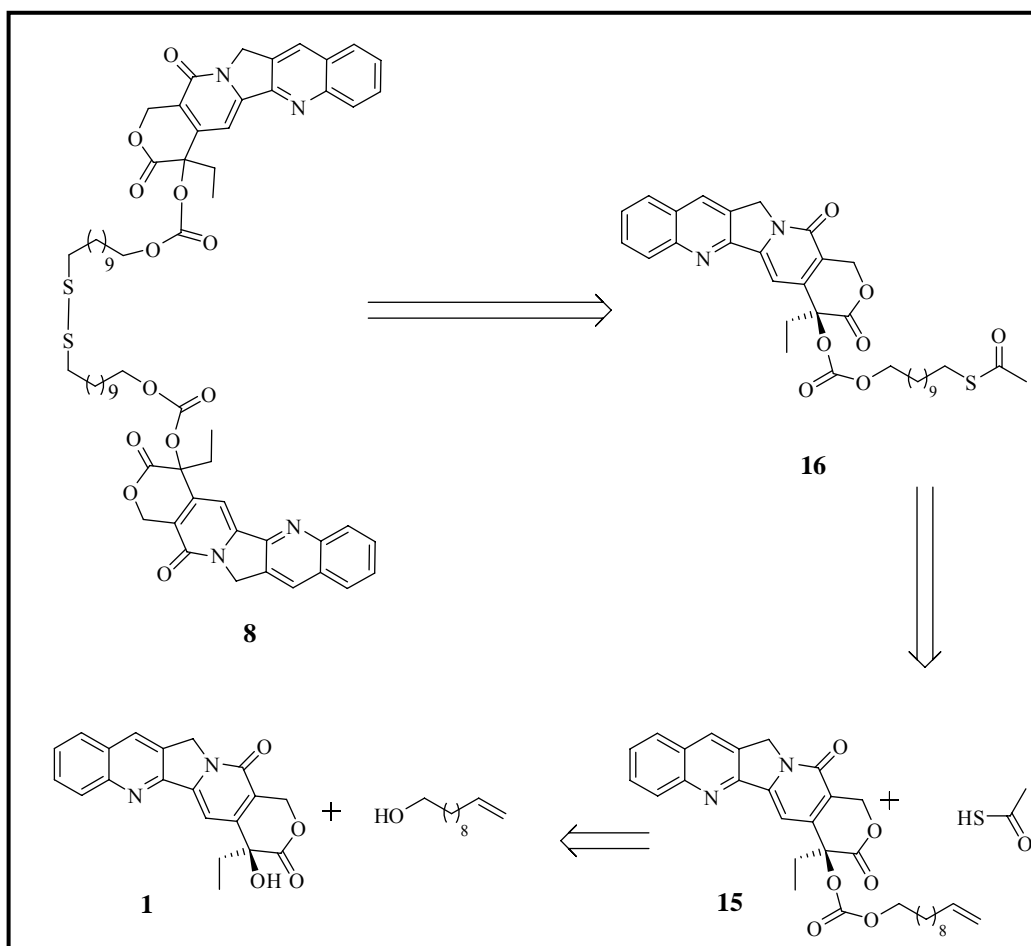
Camptothecin reacted smoothly with triphosgene in the presence of DMAP in dichloromethane to generate, in situ, the highly reactive intermediate chloroformate as it was reported by Zhao et al.[120]. The chloroformate whose formation can be determined by the appearance of pink color was then reacted readily with free linker to give the corresponding CPT-linker derivative (Figure 18).



**Figure 18.** Reactions of CPT with different linkers

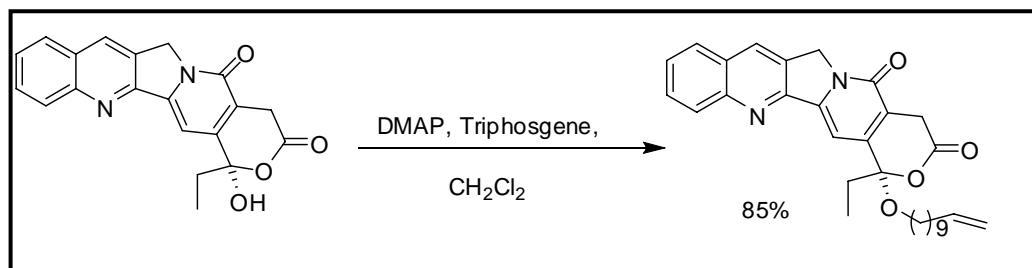
### 2.2.1. First Applied Method for the Synthesis of 20-(11, 11'-disulfaneyldiundecan)camptothecin

Figure 19 shows the first planned retro-synthetic way for the synthesis of 20-OH substituted CPT derivative **8**. Camptothecin was chosen as the starting material and it was reacted with 3 equivalent of DMAP and 0.25 equivalent of trifosgen in dichloromethane at room temperature to generate reactive intermediate chloroformate. After addition of undecenol to this solution, 20- (undec-10-en)-camptothecin (**15**) is obtained.



**Figure 19.** First planned retro-synthetic way for the synthesis of 20-OH substituted CPT derivative

The reaction is monitored by TLC (Silica gel, DCM/MeOH 98:2). After the purification of the crude product by flash column chromatography, (DCM/MeOH 98:2), the desired product 20- (undec-10-en) camptothecin (**15**) was obtained as a yellow powder in 85% yield (figure 20).



**Figure 20.** Synthesis of 20- (undec-10-en) camptothecin

The product was identified by NMR spectroscopy. The assignment of <sup>1</sup>H-NMR spectroscopy enabled us to characterize the camptothecin derivatives. The 20-hydroxy peak of a unsubstituted camptothecin appearing at 6,5 ppm as a broad singlet. The disappearance of this peak is the most important evidence of the formation of the product. The low field of the spectrum is crowded since the aromatic protons of camptothecin appear at a range between 6,5- 8,5 ppm. Another evidence of the formation of the product is peaks of undecenol appearing at a range between 5,44–1,22 ppm.

Second step of this reaction is also shown in figure 19. 20- (Undec-10-en)-camptothecin was starting material and reacted with 0,17 equivalent of azobisisobutyronitrile (AIBN) and 15 equivalent of thiolacetic acid in 1, 4-dioxane under argon atmosphere at room temperature to generate 20 -(S-11-hydroxyundecyl ethanethioate) camptothecin (**16**) [121]. The reaction is monitored by TLC but no product was obtained.

### 2.2.2. Second Applied Method for the Synthesis of 20-(11, 11'-disulfaneyldiundecan)camptothecin

The second method for synthesis of CPT derivative is shown figure 21. Our first aim was firstly synthesis of linker S-11-hydroxyundecyl ethanethioate (**6**) then synthesis of 20-(S-11-hydroxyundecyl ethanethioate)-camptothecin (**16**), and 20-(11, 11'-disulfaneyldiundecan) - camptothecin (**8**).

Undecenol was chosen as the starting material and it was reacted with 3.75 equivalents of thiolacetic acid and 0.016 equivalents AIBN in methanol to obtained S-11-hydroxyundecyl ethanethioate (**6**). [121].

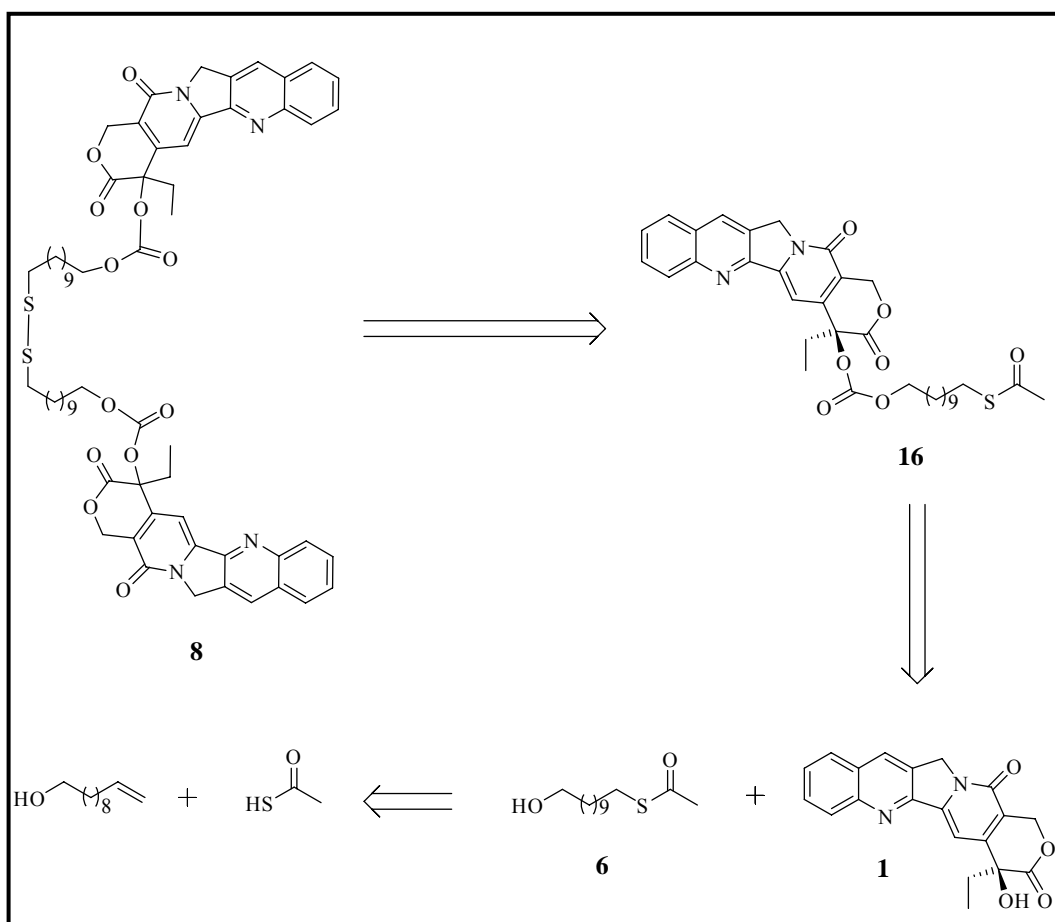


**Figure 21.** Second planned retro-synthetic way for the synthesis of 20-OH substituted CPT derivative

The reaction is monitored by TLC (Silica gel, EtOAc/Hexane 1:3). After the purification of the crude product by flash column chromatography, (EtOAc/Hexane 1:6), the desired product, S-11-hydroxyundecyl ethanethioate (**6**) was obtained as a white powder in 51 % yield (Figure 22).

The product was identified by using NMR spectroscopy. From the  $^1\text{H-NMR}$  spectrum, a singlet at 2.33 ppm from the methyl group connected to carbonyl carbon group and triplet at 3.64 ppm from  $-\text{CH}_2\text{OH}$  were obtained. From the  $^{13}\text{C-NMR}$  spectrum we observed a singlet at 195 ppm for the carbonyl carbon.

In the next step of this reaction, camptothecin was starting material and it was reacted with 3 equivalent of DMAP and 0.25 equivalent of triphosgene in dichloromethane at room temperature to generate reactive intermediate chloroformate. After addition of S-11-hydroxyundecyl ethanethioate to this solution, desired product 20-(S-11-hydroxyundecyl ethanethioate)camptothecin (**16**) is obtained.

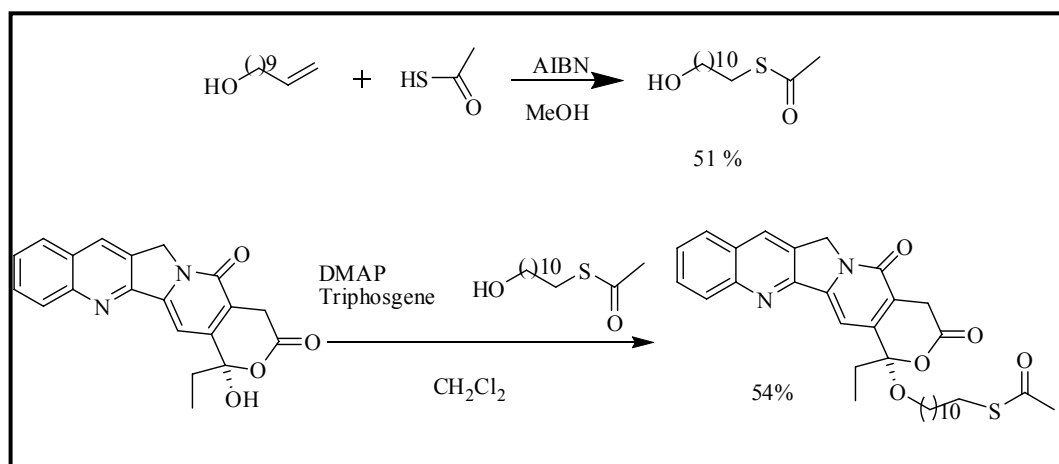


**Figure 22.** Synthesis of 20-(S-11-hydroxyundecyl ethanethioate)camptothecin

The reaction is monitored by TLC (Silica gel, DCM/MeOH 98:2). After the purification of the crude product by flash column chromatography, (DCM/MeOH 98:2), the desired product, 20-(S-11-hydroxyundecyl ethanethioate)camptothecin (**16**) was obtained as a yellow powder in 54% yield (figure 22).

The product was identified by NMR spectroscopy. The assignment of <sup>1</sup>H-NMR spectroscopy enabled us to characterize the camptothecin derivatives. The 20-hydroxy peak of a unsubstituted camptothecin appearing at 6,5 ppm as a broad singlet. The disappearance of this peak is the most important evidence of the formation of the product. The low field of the spectrum is crowded since the aromatic protons of camptothecin appear at a range between 6,5- 8,5 ppm. Another evidence of the formation of the product is peaks of 20-(S-11-hydroxyundecyl ethanethioate)camptothecin appearing at a singlet 2.33 ppm from the methyl group connected to carbonyl carbon and triplet 3.64 ppm for -CH<sub>2</sub>OH.

Dimerization of 20-(S-11-hydroxyundecyl ethanethioate) camptothecin (**16**) was last step. 20-(S-11-hydroxyundecyl ethanethioate) camptothecin (**16**) was reacted with 25% NaOMe in methanol to obtain 20- (11, 11'-disulfaneyldiundecan)camptothecin (**8**) [121]. The reaction is monitored by TLC but no product was obtained.

### **2.2.3. Third Applied Method for the Synthesis of 20-(11, 11'-disulfaneyldiundecan)camptothecin**

Our applied method is shown in figure 21. First starting from undecanol, the suitable linker 11,11'-disulfaneyldiundecan-1-ol (**7**) was synthesized. Then the CPT was reacted with this linker to obtain the desired product 20- (11,11'-disulfaneyldiundecan)camptothecin. (**8**) (figure 23).

Undecenol was chosen as the starting material and it was reacted with 3.75 equivalent of thiolacetic acid and 0.016 equivalent AIBN in methanol to obtain S-11-hydroxyundecyl ethanethioate (**6**) [121].

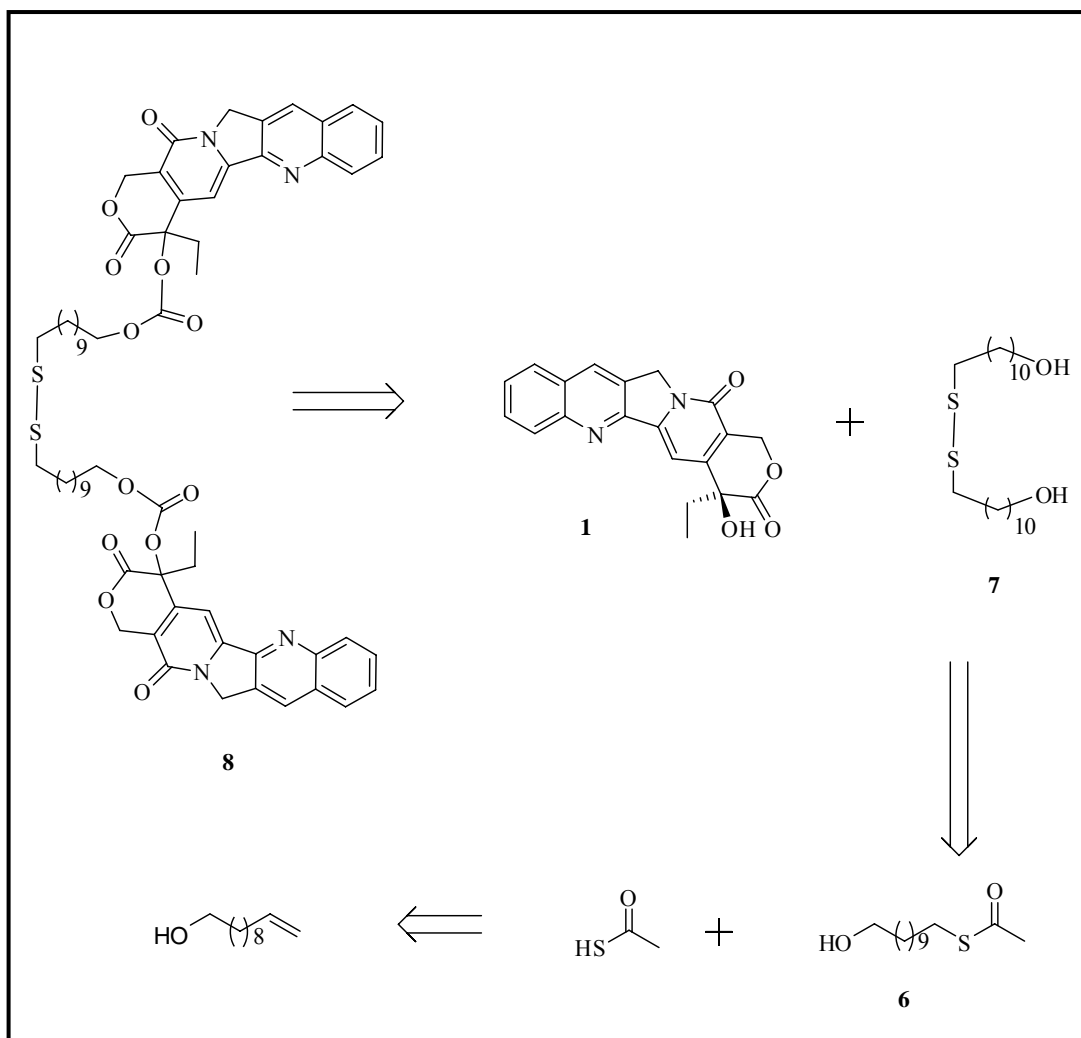


**Figure 23.** Third planned retro-synthetic way for the synthesis of 20-OH substituted CPT derivative

The reaction is monitored by TLC (Silica gel, EtOAc/Hexane 1:3). After the purification of the crude product by flash column chromatography, (EtOAc/Hexane 1:6), the desired product, S-11-hydroxyundecyl ethanethioate (**6**) was obtained as a white powder in 50% yield (figure 24).

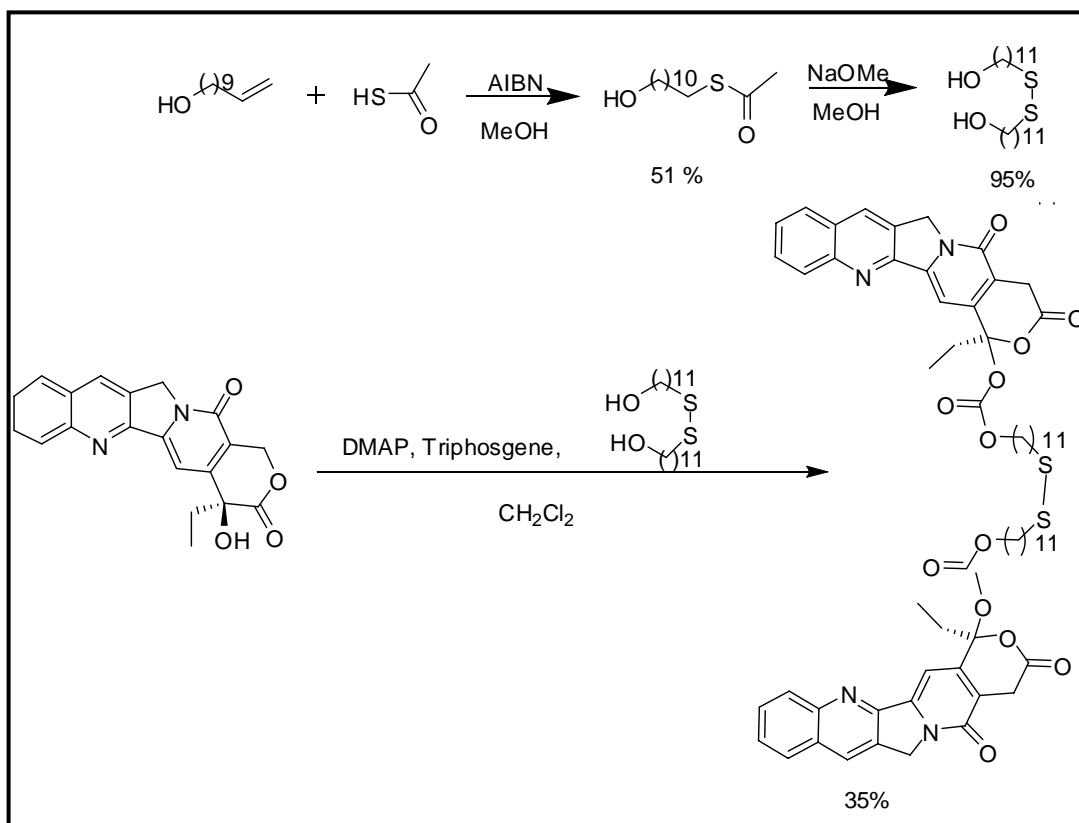


**Figure 24.** Synthesis of 20-(11,11'-disulfaneyldiundecan)captopthecin

The reaction is monitored by TLC (Silica gel, EtOAc/Hexane 1:3). After the purification of the crude product by flash column chromatography, (EtOAc/Hexane 1:6), the desired product, S-11-hydroxyundecyl ethanethioate (**6**) was obtained as a white powder in 50% yield (figure 24).

The product was identified by using NMR spectroscopy. From the <sup>1</sup>H-NMR spectrum, a singlet at 2.33 ppm for the methyl group connected to carbonyl carbon and triplet at 3.64 ppm from -CH<sub>2</sub>OH were observed. From the <sup>13</sup>C-NMR spectrum we observed a singlet at 195 ppm for the carbonyl carbon was observed.

In the next step of this reaction, S-11-hydroxyundecyl ethanethioate (**6**) was reacted with 25% NaOMe in methanol to obtain 11, 11'-disulfaneyldiundecan-1-ol (**7**) [121].

The reaction was monitored by TLC (Silica gel, DCM/MeOH 98:5). After the purification of the crude product by flash column chromatography, (DCM/MeOH 95:5), the desired product, 11, 11'-disulfaneyldiundecan-1-ol (**7**) was obtained as a white powder in 95% yield (Figure 24).

The product was identified by using NMR spectroscopy. From the <sup>1</sup>H-NMR spectrum, a triplet at 3.62 ppm from the –CH<sub>2</sub>OH group and another triplet at 2.64 from the –CH<sub>2</sub>S– group were observed.

In the last step of this method, camptothecin was starting material and reacted with 3 equivalent of DMAP and 0.25 equivalent of triphosgene in dichloromethane at room temperature to generate reactive intermediate chloroformate. After addition of 11,11'-disulfaneyldiundecan-1-ol (**7**) to this solution, desired product 20- (11,11'-disulfaneyldiundecan)camptothecin (**8**) was obtained.

The reaction was monitored by TLC (Silica gel, DCM/MeOH 98:2). After the purification of the crude product by flash column chromatography, (DCM/MeOH 98:2), the desired product, 20- (11, 11'-disulfaneyldiundecan)camptothecin was obtained as a yellow powder in 35 % yield (Figure 24).

The product was identified by NMR spectroscopy. The assignment of <sup>1</sup>H-NMR spectroscopy enabled us to characterize the camptothecin derivatives. The 20-hydroxy peak of a unsubstituted camptothecin appears at 6,5 ppm as a broad singlet. The disappearance of this peak is the most important evidence of the formation of the product. The low field of the spectrum is crowded since the aromatic protons of camptothecin appear at a range between 6,5- 8,5 ppm. Another evidence of the formation of the product is peaks of 20-(11, 11'-disulfaneyldiundecan)camptothecin appearing at 2,56 ppm as a triplet from methyl group connected with linker carbonyl carbon and broad peaks a range between 1.54 – 1.22 ppm from alkyl group the linker.

As it was mentioned several times before, the selective targeting of a compound to tumors, or for that matter to any structure in the body, requires high stability of the compound in blood. Stability was already the goal of the study so, the stability of the new compounds was investigated.

The most currently used analytical method for camptothecin derivatives is spectrofluorimeter. The fluorometric detection method show high sensitivity due the high fluorescence feature of the totally planar pentacyclic structure of camptothecin. The hydrolysis of the lactone moiety in camptothecin is also routinely monitored by using spectrofluorimeter. Understanding the pharmacokinetic and pharmacodynamic parameters of lactone ring opening requires methodologies that allow quantitation of the intact lactone species, total drug concentrations and preferably, carboxylate levels as well.

Ring substitutions influence the pentacyclic chromophore of CPT and can modify its spectra. This effect on spectra of CPT should be considered in order to understand the state of the molecule at given experimental conditions (pH, solvent polarity, ionic strength, molecular environment, etc.). Spectral identification of these effects should validate the measurements of the pH-dependent hydrolysis reactions. Moreover, as it will be shown below, the spectral patterns can be useful to differentiate not only the lactone and carboxylate forms of CPT but also the interconvertible derivatives.

Kinetic measurements were performed in a 1 cm quartz cell, placed in a spectrofluorimeter. Tris buffer, pH 5,5, 7,4 or 9,4 was thermostated in the cell at room temperature before dilution of the drug in it and temperature was kept constant during the measurements. The pH was controlled before and after the kinetic measurements. The measurements were started ( $t_s=0$ ), when stock solution of the drug in DMSO was diluted in buffer. In order to follow the opening of the lactone ring in CPTs, fluorescence emission spectra were recorded with time intervals varying from 2 to 16 min, depending on the rate of reaction.

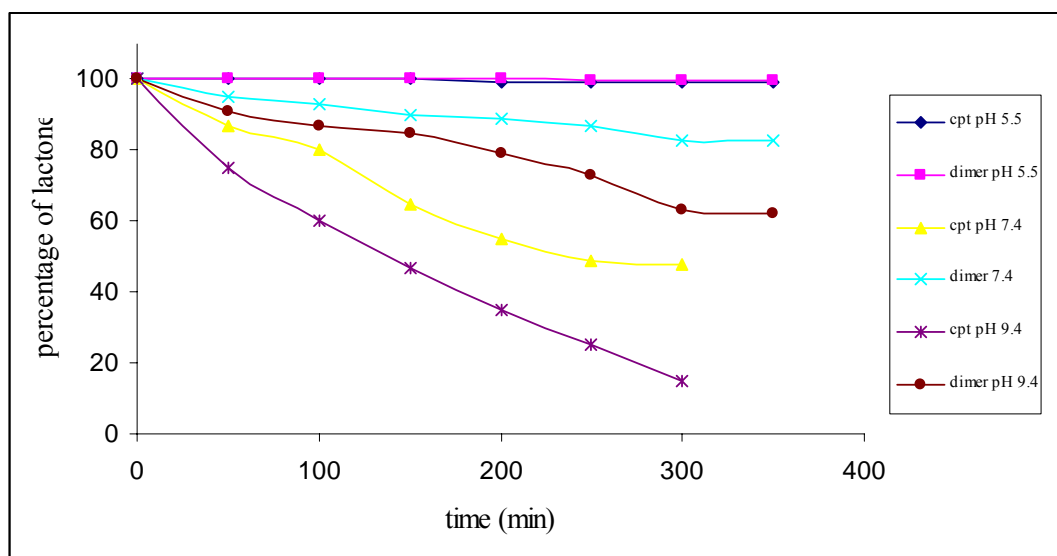


**Figure 25.** Percentage of lactone CPT and - (11, 11'-disulfanediyldiundecan) – captothecin graph

**Cpt pH 5.5** : CPT in pH 5.5 buffer solution

**Dimer pH 5.5:** 20- (11, 11'-disulfanediyldiundecan)captothecin in pH 5.5 buffer solution

**Cpt pH 7.4** : CPT in pH 7, 4 buffer solution

**Dimer pH 7.4:** 20- (11, 11'-disulfanediyldiundecan)captothecin in pH 7.4 buffer solution

**Cpt pH 9.4** : CPT in pH 9, 4 buffer solution

**Dimer pH 9.4:** 20- (11, 11'-disulfanediyldiundecan) captothecin in pH 9.4 buffer solution

The time needed for recording one spectrum was about 20 s. For a given derivative, emission was excited with a wavelength, corresponding to the long-wavelength maximum in the excitation spectrum of the lactone form: 370nm for CPT. Hydrolysis reactions were monitored via the evolution, as a function of time, of the ratio of the fluorescence intensities at two different wavelengths. The choice of these wavelengths came from the fact that they provide the most significant difference in the intensity ratio in the spectra of pure lactone and carboxylate forms. The intensities, characteristic for the pure lactone and pure carboxylate forms of each derivative have been measured before the kinetic study and thereafter used as constants.

It is clear that, modification of CPT at the 20<sup>th</sup> enhances the drug stability: by 1,5 hours at pH 7,4 CPT lactone level fell less than 60% whereas 20 - (11, 11'

disulfanediylundecan) – camptothecin lactone level reached only 89% at the same time.

As a result, this part of the camptothecin study was successfully completed. The substituents were successfully connected to camptothecin through the 20- hydroxyl functionality which provides the protection of hydroxyl group. The substituents have also improved the solubility and stability of camptothecin which were the most important handicap in its applications.

### **2.3. Synthesis of Gold Nanoparticles and 20-(11, 11'-disulfanediylundecan) - camptothecin Derivative coated Gold Nanoparticles**

Generally, gold nanoparticles are produced in a liquid ("liquid chemical methods") by reduction of hydrogen tetrachloroaurate ( $\text{HAuCl}_4$ ), although more advanced and precise methods do exist. After dissolving  $\text{HAuCl}_4$ , the solution is rapidly stirred while a reducing agent is added. This causes  $\text{Au}^{3+}$  ions to reduce to un-ionized gold atoms. As more and more of these gold atoms form, the solution becomes supersaturated, and gold gradually starts to precipitate in the form of sub-nanometer particles. The rest of the gold atoms that form stick to the existing particles, and, if the solution is stirred vigorously enough, the particles will be fairly uniform in size.

To prevent the particles from aggregating, some sort of stabilizing agent that sticks to the nanoparticle surface is usually added. They can be functionalized with various organic ligands to create organic-inorganic hybrids with advanced functionality [122].

Pioneered by J. Turkevich et al. in 1951 and refined by G. Frens in 1970s, this recipe is the simplest one available [123]. Generally, it is used to produce modestly monodisperse spherical gold nanoparticles suspended in water of around 10–20 nm in diameter. Larger particles can be produced, but this comes at the cost of monodispersity and shape.

$\text{HAuCl}_4$  was dissolved in deionized water and heated until boiling. While it was continued heating and stirring vigorously, add 0.5% sodium citrate solution in water

and keep stirring for next 30 minutes. The colour of the solution changed gradually from faint yellowish to clear to grey to purple to deep purple, until settling on wine-red. This colour shows that gold nanoparticles are obtained.

The sodium citrate first acts as a reducing agent. Later the negatively-charged citrate ions are adsorbed onto the gold nanoparticles, introducing the surface charge that repels the particles and prevents them from aggregating.

Brust et. al. discovered another method for the experimental generation of gold particles[124]. This method was applied in this study.

Preparation of colloidal metals in a two-phase system was introduced by Faraday, who reduced an aqueous gold salt with phosphorus in carbon disulfide and obtained a ruby coloured aqueous solution of dispersed gold particles. Combining this two-phase approach with the more recent techniques of ion extraction and monolayer selfassembly with alkane thiols a one-step method for the preparation of an unusual new metallic material of derivatised nanometre-sized gold particles is described.

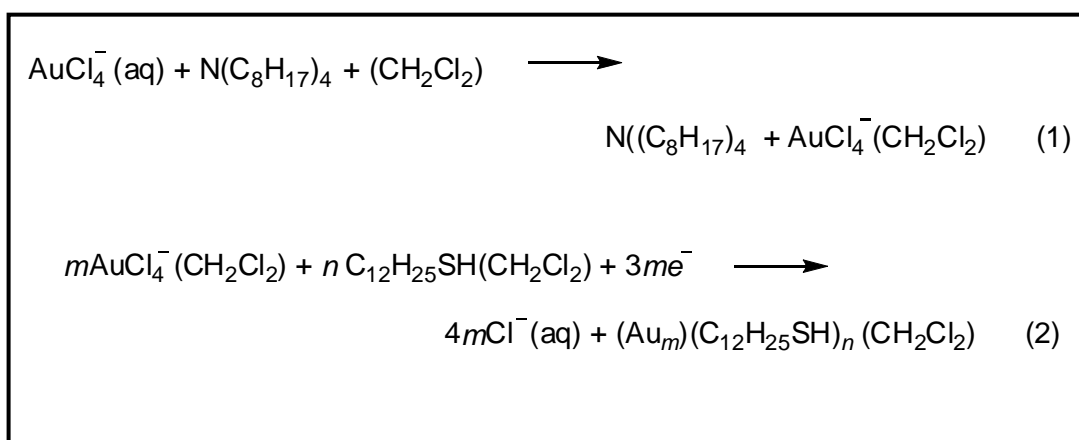


**Figure 26.** Synthesis of gold nanoparticles

Two phase redox reactions can be carried out by an appropriate choice of redox reagents present in the adjoining phases [125]. In the present case,  $\text{AuCl}_4^-$  was transferred from aqueous solution to dichloromethane (or toluene) using tetraoctylammonium bromide as the phase-transfer reagent and reduced with

aqueous sodium borohydride in the presence of dodecanethiol ( $C_{12}H_{25}SH$ ). On addition of the reducing agent, the organic phase changes colour from orange to deep brown within a few seconds. The overall reaction is summarized by equation. (1) and (2), where the source of electrons is  $BH_4^-$ .

The UV-VIS spectrum of the gold nanoparticles solution was obtained as expected (Figure 25). There was a peak at 520 nm for bare gold nanoparticles.

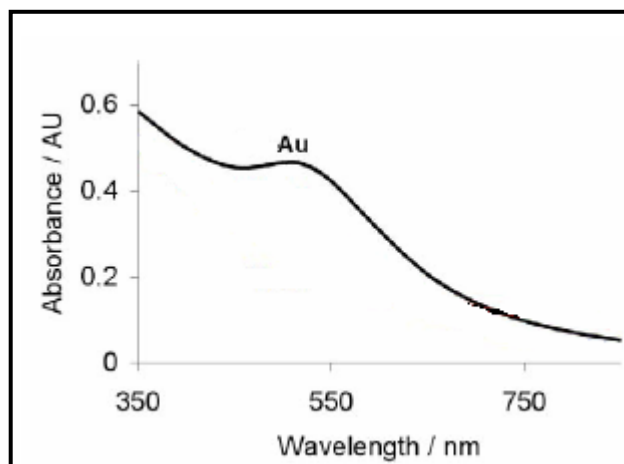


**Figure 28:** UV-VIS Spectrum of the Gold Nanoparticles

The preparation technique was as follows (Figure 24). An aqueous solution of hydrogen tetrachloroaurate was mixed with a solution of tetraoctylammonium bromide in dichloromethane. The two-phase mixture was vigorously stirred until all the tetrachloroaurate was transferred into the organic layer and 20-(11'-disulfaneyldiundecan)- camptothecin derivative was then added to the organic phase. A freshly prepared aqueous solution of sodium borohydride was slowly added with vigorous stirring. After further stirring for 3 h the organic phase was separated, evaporated to 10 mL in a rotary evaporator and mixed with 400 mL ethanol to remove excess thiol. The mixture was kept for 4 h at  $-18\text{ }^{\circ}C$  and the dark brown precipitate was filtered off and washed with ethanol.

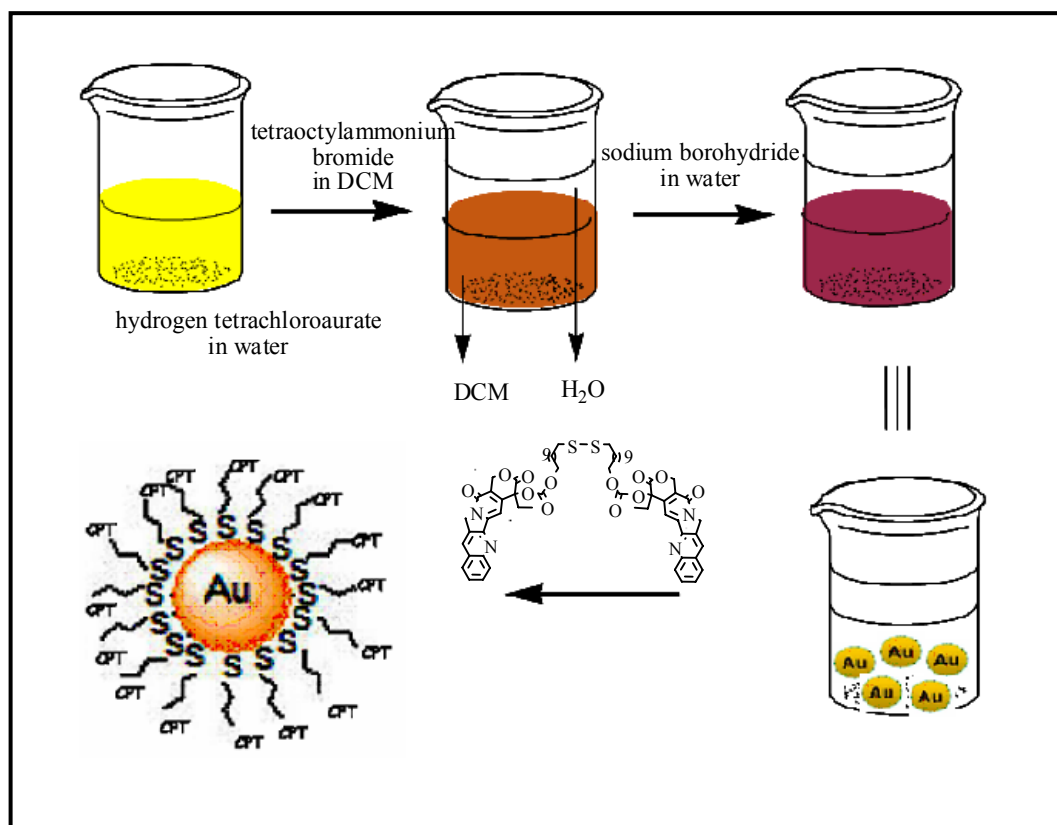


**Figure 27:** Synthesis of 20-(11, 11'-disulfaneyldiundecan) - Camptothecin Derivative coated AuNPs

The product was identified by NMR spectroscopy. The assignment of  $^1\text{H-NMR}$  spectroscopy enabled us to characterize the gold nanoparticles coated with 20-(11'-11 disulfaneyldiundecan)- camptothecin derivatives. The peaks due to gold nanoparticles coated with 20-(11, 11'-disulfaneyldiundecan)- camptothecin derivative are same 20-(11,11'-disulfaneyldiundecan)- camptothecin derivative but all of peaks are broad because of gold nanoparticles.

. The fluorometric detection method was also made for 20-(11, 11'-disulfaneyldiundecan)camptothecin coated gold nanoarticles. Kinetic measurements were same which performed 20-(11, 11'-disulfaneyldiundecan)camptothecin conditions.

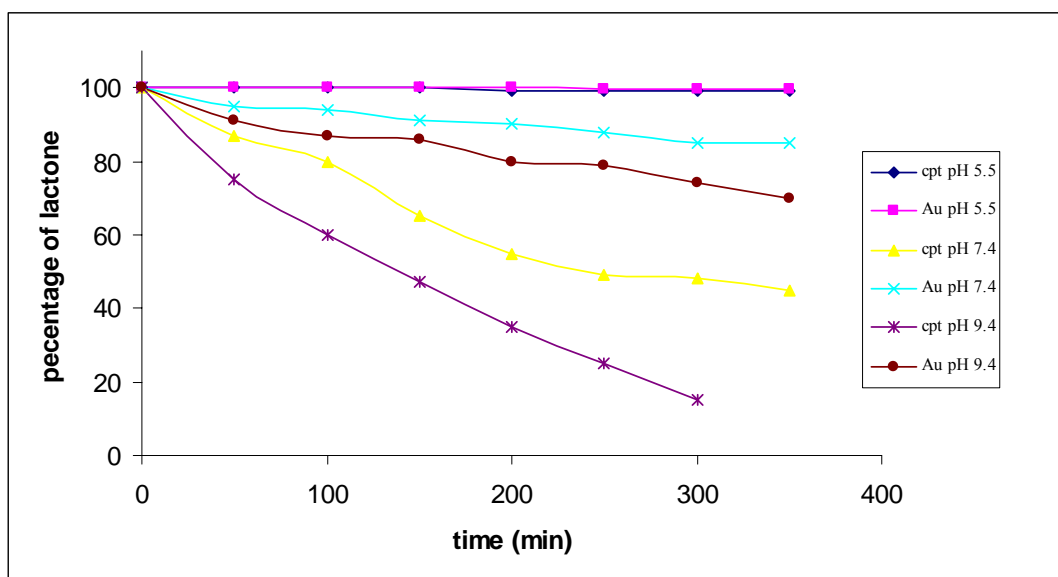


**Figure 29.** Percentage of lactone CPT and 20 - (11, 11'-disulfanediyldiundecan) – camptothecin coated AuNPs graph

**Cpt pH 5.5 :** CPT in pH 5.5 buffer solution

**Au pH 5.5 :** 20- (11, 11'-disulfanediyldiundecan)camptothecin coated AuNPs in pH 5.5 buffer

**Cpt pH 7.4:** CPT in pH 7, 4 buffer solution

**Au pH 7.4 :** 20- (11, 11'-disulfanediyldiundecan)camptothecin coated AuNPs in pH 7.4 buffer

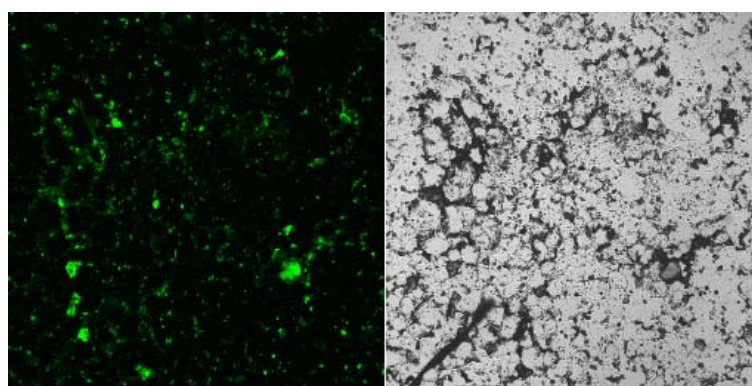
**pH 9.4:** CPT in pH 9, 4 buffer solution

**Au pH 9.4 :** 20- (11, 11'-disulfanediyldiundecan) camptothecin coated AuNPs in pH 9.4 buffer

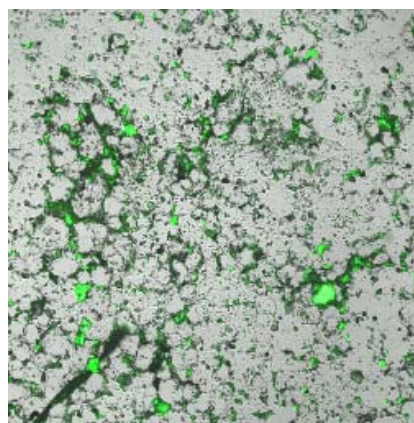
It is clear that, connection of CPT on AuNPs surface increase the drug stability: by 1,5 hours at pH 7,4 CPT lactone level fell less than 60% whereas 20-(11, 11' disulfanediyldiundecan)camptothecin lactone level reached only 90% at the same time.

As a result, the camptothecin coated AuNPs study was succesfully completed. The drug were successfully connected to AuNPs surface which provides the protection of drug stability. This work provides a solution to the most important handicap in camptothecin applications.

We also took confocal microscopie image of 20-(11, 11'-disulfanediyldiundecan)camptothecin coated gold nanoarticles (Figure 27).



(a) Only fluorescence image (b) Only white light image



(c) Both fluorescence and white light image

**Figure 30:** Confocal Microscope Image of 20-(11, 11'-disulfanediyldiundecan)camptothecin Coated Gold Nanoarticles

Using by confocal microscope, an experiment was done. 20-(11,11'-disulfanediyldiundecan)- camptothecin derivative coated gold nanoparticles is soluble in DCM but not soluble in ethanol. 20-(11, 11'-disulfanediyldiundecan)camptothecin is both soluble in ethanol and DCM. The sample was prepared and ethanol was dropped on this sample. After taking image for 15 minute, there was no change at sample. If the sample was not 20-(11,11'-disulfanediyldiundecan)camptothecin derivative coated gold nanoparticles, it would have spread. This experiment also shows that 20-(11,11'-disulfanediyldiundecan)camptothecin derivative coated gold nanoparticles were synthesized.

We also took transmission electron microscopy (TEM) image of 20-(11'-disulfaneyldiundecan)camptothecin coated gold nanoarticles (Figure 28).

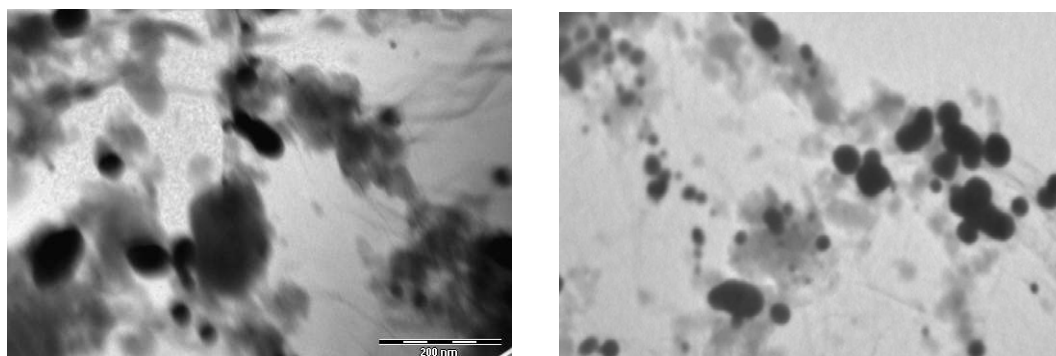


**Figure 31:** TEM Image of 20-(11'-disulfaneyldiundecan)camptothecin Coated Gold Nanoarticles

TEM images show that 20-(11'-disulfaneyldiundecan)camptothecin coated gold nanoarticles are about 40 nm.

## CHAPTER 3

### EXPERIMENTAL

The compounds in this study were identified by the instruments mentioned below.

Proton and carbon-13 nuclear magnetic resonance spectra ( $^1\text{H}$  NMR /  $^{13}\text{C}$  NMR) were recorded on Bruker Spectrospin Avance DPX 400 spectrometer in  $\text{CDCl}_3$ . Chemical shifts are given in parts per million (ppm) downfield from tetramethyl silane as the internal standard. Spin multiplicities are mentioned as: s (singlet), d (doublet), dd (doublet of doublet), t (triplet), m (multiplet).

TLC was carried out on aluminium sheets precoated with silica gel 60F254 (Merck) and the spots were visualized with UV light ( $\lambda=254$  nm).

Column chromatography was performed on Biotage combi flash. The relative proportion of solvents are in volume: volume ratio used in column chromatography as eluent.

Solvents were either in technical or high grade and when necessary they were dried with appropriate drying agents and purified by distillation. DCM was distilled over calcium hydride.

### 3.1. General Procedure for the Synthesis of S-11-hydroxyundecyl ethanethioate (6)

A solution of undec-10-en-1-ol (1,36 g, 8 mmol) in 30 mL MeOH was treated with 30 mmol (2,3 g, 2,3 mL) of freshly distilled thioacetic acid. The solution was purged with argon for 20 min and 10 mg of AIBN was added. The reaction was irradiated with 360 nm light overnight, quenched with 1 mL of cyclohexene and evaporated. The residue was purified by combi flash EtOAc/Hexane 1:6 to afford 690 mg (51%) of S-11-hydroxyundecyl ethanethioate (6) as a white powder.

$^1\text{H}$  NMR ( $\text{CDCl}_3$ )  $\delta$  3.64 (2H, t,  $J=6.6$  Hz), 2.87 (2H, t,  $J=7.3$  Hz), 2.33 (3H, s), 1.54–1.59 (6H, broad), 1.30–1.37 (12H, broad).

$^{13}\text{C}$  NMR ( $\text{CDCl}_3$ )  $\delta$  25.8, 29.1, 29.5, 30.5, 32.8, 62.9, 76.6, 77.2, 195.1.

### 3.2. General Procedure for the Synthesis of 11,11'-disulfanediyldiundecan-1-ol (7)

A solution of S-11-hydroxyundecyl ethanethioate (105 mg 0.43 mmol) in 5 mL of MeOH was treated with 30  $\mu\text{L}$  of 25% (w/v) NaOMe/ MeOH. The reaction was stirred at room temperature for 24 h with a slow flow of air bubbling through the solution. Methanol was evaporated and the residue was purified by combi flash DCM/MeOH 95:5 to afford 83 mg (95 %) of 11, 11'-disulfanediyldiundecan-1-ol (7) as a white powder.

$^1\text{H}$  NMR ( $\text{CDCl}_3$ )  $\delta$  3.55 (4H, t,  $J=6.56$  Hz), 2.59 (4H, t,  $J=7.38$ ), 1.60 (4H, h,  $J=7.35$  Hz), 1.48 (8H, h,  $J=6.98$ ), 1.22 (24H, broad).

$^{13}\text{C}$  NMR ( $\text{CDCl}_3$ )  $\delta$  77.2, 62.8, 39.1, 32.8, 29.6, 29.5, 29.4, 29.2, 28.5, 25.7.

### 3.3. General Procedure for the Synthesis of 20-(undec-10-en)camptothecin (16)

A suspension of camptothecin (139 mg 0.40 mmol), triphosgene (44 mg 0.147 mmol), 156 mg (1.28 mmol) DMAP in 20 mL anhydrous DCM was stirred for 10 minutes. Undec-10-en-1-ol (68 mg, 0.40 mmol) was added and the reaction stirred

over night. The residue was purified by combi flash DCM/MeOH 98:2 to afford 151 mg (85%) of 20-( undec-10-en)- camptothecin (**16**) as a yellow powder.

<sup>1</sup>H NMR 8.30 (1H, s), 8.14 (1H, d, J=8.5), 7.84 (1H, d, J= 7.8 Hz), 7.75 (1H, t, J=7.9 Hz), 7.58 (1H, t, J=7.49), 7.22 (1H,s), 7.19 (1H, s), 5.68 (1H,m),5.59 (1H, apart of AB system J=15 Hz), 5.31 (1H, apart of AB sytem, J=15 Hz), 5.19(2H, s), 4.89 (1H,s), 4,83 (1H, t, J=10,22 Hz), 4.10-3.96 (2H, m), 1.86-1.92 (2H,m), 1.14 (16 H, broad), 0.94 (3H, t, J=7.41 Hz).

### **3.4. General Procedure for the Synthesis of 20-( S-11-hydroxyundecyl ethanethioate)camptothecin (17)**

A suspension of camptothecin (139 mg 0.40 mmol), triposgene (44mg 0,147 mmol), 156 mg (1.28 mmol) DMAP in 20 mL anhydrous DCM was stirred for 10 minute. S-11-hydroxyundecyl ethanethioate (98 mg, 0.40 mmol) was added and the reaction stirred over night. The residue was purified by combi flash DCM/MeOH 98:2 to afford 109 mg (54%) of 20-( S-11-hydroxyundecyl ethanethioate)-camptothecin (**17**) as a yellow powder.

<sup>1</sup>H NMR (CDCl<sub>3</sub>) 8.36 (1H, s), 8.21 (1H, d, J=8.51), 7.91(1H, d, J= 8.1 Hz), 7,82 (1H, t, J=7.2 Hz), 7.65 (1H, t, J=7.32), 7.28 (1H,s), 7.26 (1H, s), 5.58 (1H, apart of AB system J=17 Hz), 5.28 (1H, apart of AB sytem), 5.27(2H, s), 4.04-4.15 (2H broad), 2.82 (2H, t, J=7.32), 2.30 (3H, s), 1.54-1.59 (6H,broad), 1.30-1.37 (12H broad), 1.01 (3H, t, J=7.5 Hz).

### **3.5. General Procedure for the Synthesis of 20-( 11,11'-disulfanediyldiundecan)camptothecin (8)**

A suspension of camptothecin (139 mg 0.40 mmol), triposgene (44mg 0,147 mmol), 156 mg (1.28 mmol) DMAP in 20 ml anhydrous DCM was stirred for 10 minute. 11, 11'-disulfanediyldiundecan-1-ol (81 mg, 0.40 mmol) was added and the reaction stirred over night. The residue was purified by combi flash DCM/MeOH

98:2 to afford 65 mg (35%) of 20-(11'-disulfanediyldiundecan)- camptothecin (**8**) as a yellow powder.

<sup>1</sup>H NMR (CDCl<sub>3</sub>) 8.41 (2H, s), 8.18 (2H, d, J=8.2 Hz), 7.84 (2H, d, J=8.1), 7.73 (2H, t, J=8.2), 7.2 (2H, t, J=7.3), 5.59 (2H apart of AB system), 5.29 (2H apart of AB system), 5.22 (4H, s), 3.4 (4H, broad), 2.56 (4H, t, J=7.38 Hz), 2.26-2.21 (4H, m), 2.19-2.14 (12 H, m), 1.22 (24H, broad), 1.01 (6H, t, J=7,76)

### **3.6. General Procedure for the Synthesis 20-(11, 11'-disulfanediyldiundecan)camptothecin coated Gold Nanoparticles**

An aqueous solution of hydrogen tetrachloroaurate (30 ml, 30 mmol dm<sup>-3</sup>) was mixed with a solution of tetraoctylammonium bromide in DCM (80 ml, 50 mmol dm<sup>-3</sup>). The two-phase mixture was vigorously stirred until all the tetrachloroaurate was transferred into the organic layer and of 20-(S-11-hydroxyundecyl ethanethioate)- camptothecin (170 mg) was then added to the organic phase. A freshly prepared aqueous solution of sodium borohydride (25 ml, 0,4 mol dm<sup>-3</sup>) was slowly added with vigorous stirring. After further stirring for 3 h the organic phase was separated, evaporated to 10 ml in a rotary evaporator and mixed with 400 ml ethanol to remove excess thiol. The mixture was kept for 4 h at -18 °C and the dark brown precipitate was filtered off and washed with ethanol. The crude product was dissolved in 10 ml DCM and again precipitated with 400 ml ethanol.

## CHAPTER 4

### CONCLUSION

Many therapeutic drugs have undesirable properties that may become pharmacological, pharmaceutical, or pharmacokinetic barriers in clinical drug application. Among the various approaches to minimize the undesirable drug properties while retaining the desirable therapeutic activity, the chemical approach using drug derivatization offers perhaps the highest flexibility and has been demonstrated as an important means of improving drug efficacy. There are many efforts for the modification of camptothecin to obtain new derivatives addressing the solubility and stability problems. It was also the aim of this study to synthesize new camptothecin derivatives possessing high solubility and high stability but less toxicity.

In the first part of the study a targeted prodrug approach was modified on camptothecin drug. The 20-OH functional group of camptothecin was replaced with a alkyl derivative containing thiol group. The new prodrugs should be more stable than camptothecin itself since the protection of 20-OH provides stabilization. The synthesis of the aimed prodrug was achieved after several steps and the new prodrugs possessed higher stability as expected.

In the second part of the study gold nanoparticles were synthesized and the camptothecin derivative containing thiol group at 20-OH position was connected to the gold surface.

## REFERENCES

1. American Cancer Society. *Cancer Facts & Figures 2007*. Atlanta: American Cancer Society; **2007**.
2. Dolmans, DE.; Fukumura D., Jain RK. , *Nat Rev Cancer*, **2003**, 3 ,380.
3. Stewart CF, Zamboni WC, Crom Wret al. *Invest New Drugs* **1996**, 14, 37
4. Sawada, S.; Okajima, S.; Aiyama, R.; Nokota, K.; Furuta, T.; Yokokura, T.; Sugino, E.; Yamaguchi, K.; Miyasaka, T. *Chem. Pharm. Bul.* **1991**, 39, 1446.
5. Wall ME, Wani MC, Cook CE. *J Am Chem Soc* **1966**, 88, 3888
6. Fassberg, J.; Stella, V. J. *J. Pharm. Sci.* **1992**, 81, 676.
7. Burke, T. G.; Mi, Z. *Anal. Biochem.* **1993**, 212, 285.
8. Moertel, C. G.; Schutt, A. J.; Reitemeier, R. J.; Hahn, R. G. *Cancer Chemother. Rep.* **1972**, 56, 95.
9. Gottlieb, J. A.; Luce, J. K. *Cancer Chemother. Rpt.* **1972**, 56, 103.
- 10 Hertzberg, R.P.; Caranfa, M.J.; Holdeng, K.G.; Jakas, D.R., G Gallagher, M.R. Mattern, S.M. Mong, J.O. Bartus, R.K. Johnson, W.D. Kingsbury, *J. Med. Chem*, **1989**, 32, 715.
11. C. Jaxel, K.W. Kohn, M.C. Wani, M.E. Wall, Y. Pommier, *Cancer Res.* **1989**, 49, 1465
12. Y.H. Hsiang, L.F. Liu, M.E.Wall, M.C.Wani, A.W. Nicholas, G. Manikumar, S. Kirschenbaum, R. Silber, M. Potmesil *Cancer Res.* **1989**, 49, 4385.
13. Y. Pommier, C. Jaxel, D. Kerrigan, K.W. Kohn, in: M. Potmesil, K.W. Kohn (Eds.), *DNA Topoisomerases and Cancer*, Oxford University Press, New York, **1991**, 121.
14. M. Potmesil, *Cancer Res.* **1994**, 54, 1431.
15. J. Fassberg, V.J. Stella, *J. Pharm. Sci.* **1992**, 81, 676.
16. T.G. Burke, Z. Mi, *Anal. Biochem.* **1993** 212, 285.
17. T.G. Burke, C.B. Munshi, Z. Mi, Y. Jiang, *J. Pharm. Sci.* **1995** , 84, 518.
18. W.J.M. Underberg, R.M.J. Goossen, B.R. Smith, *J. Pharm. Biomed. Anal.* **1990**, 8, 681.
19. VJaxel, C.; Kohn, K. W.; Wani, M. C., et al. *Cancer Res.*, **1989**, 49, 1465.

20. Luzzio, M. J.; Besterman, J. M.; Emerson, D. L.; Evans, M. G.; Lackey, K.; Leitner, P. L.; McIntyere, G.; Morton, B.; Myers, P. L.; Peel, M.; Sisco, J. M.; Sternbach, D. D. Tong, W. Q.; Truesdale, A.; Uehling, D. E.; Vuong, A.; Yates, J. J. *Med. Chem.* **1995**, 38, 395.
21. Emerson, D. L.; Besterman, J. M.; Brown, H. R.; Evans, M. G.; Leitner, P. L.; Luzzio, M. J.; Shaffer, J. E.; Sternbach, D. D.; Uehling, D. E.; Vuong, A. J. *Cancer Res.* **1995**, 55, 603.
22. Kingsbury WD, Boehm JC, Jakas DR, et al. *J Med Chem* **1991**; 34, 98.
23. Houghton PJ, Cheshire PJ, Myers L, Stewart CF, Synold TW, Houghton JA. *Cancer Chemother Pharmacol* **1992**; 31, 229.
- 24 Saltz L, Sirott M, Young C, et al. *J Natl Cancer Inst* **1993**; 85, 1499.
25. Vladu, B.; Woynarowski, J.; Manikumar, G.; Wani, M.; Wall, M.; Von Hoff, D.; Wadkins, R.; *Molecular Pharmacology*, **2000**, 57, 243.
26. C. Bailly , *Critical Reviews in Oncology/Hematology* **2003**, 45, 9192 \_
27. Osheroff, N. *Pharmacol. Ther.* **1989**. 41
28. Gupta, M.; Fujimori, A.; Pommier, Y. *Biochim. Biophys. Acta* **1995**, 1262, 29..  
Hsieh, T. *Curr. Opin. Cell. Biol.* **1992**, 4, 396.
30. Osheroff, N.; Zecherich, E. L.; Gale, K. C. *BioEssays* **1991**, 13, 269
31. Liu, F. L.; *Annu. Rev. Biochem.* **1989**, 58, 351
32. Holden, J. A. *Curr. Med. Chem.-Anti-Cancer Agents* **2001**, 1,1.
33. Bailly, C. *Crit. Rev. Oncol./Hematol.* **2003**, 45, 91.
34. Yang Z, Champoux JJ, *J Biol Chem*, **2001**; 276, 677.
35. a) Wang, J. C. *Annu. Rev. Biochem.* **1996**, 65, 635. (b) Wang, J. C. Q. *Rev. Biophys.* 1998, 31, 107. (c) Pommier, Y. *Biochimie*, **1998**, 80, 255. (d) Champoux, J. J. *Ann. J. M.*; Jerina, D. M.; Pommier, Y. *Biochemistry*, **2002**, 41, 1428.
36. Hsiang, Y.-H.; Hertzberg, R.; Hecht, S.; Liu, L. F. *J. Biol. Chem.* **1985**, 260, 14873.
37. Hsiang, Y.-H.; Lihou, M. G.; Liu, L, F. *Cancer Res.* **1989**, 49,5077.
38. Nitiss, J. and Wang J. C., *Proc. Natl. Acad. Sci. U.S.A.*, **1987**, 84, 7501.
39. Andoh, T., Ishii, K., Suzuki, Y., Ikegami, Y., Kusunoki, Y., Takemoto, Y., and Okada, K., *Proc. Natl. Acad. Sci. U.S.A.*, **1987**, 5565.
40. Hsiang, Y.-H., Lihou, M. G., and Liu, L. F., *Cancer Res.*, **1989**, 49, 5077.

41. Holm, C., Covey, J. M., Kerrigan, D., and Pommier, Y., *Cancer Res.*, **1990**,50, 5919.
42. D' Arpa, P., and Liu. F., *Cancer Res.* **1990**, 50, 6919.
43. Tsao, Y. P.; D' Arpa, P.; Liu, L. F.; *Cancer Res.*, **1992**, 52, 1823.
44. Redinbo, M. R.; Stewart, L.; Kuhn, P.; Champoux, J. J.; Hol, W. G. *J. Sci.* **1998**, 279, 1504.
45. Padlan, E. A.; Kabat, E. A. *Methods Enzymol.* **1991**, 203, 3-21.
46. Stork, G.; Schultz, A.G. *J. Am. Chem. Soc.* **1971**, 93, 4074.
47. Pilch, D. S.; Kerrigan, J. E.; *Biochemistry*, **2001**, 40, 9792
48. Richard Feynman There's Plenty of Room at the Bottom. An Invitation to Enter a New Field of Science, lecture, annual meeting of the American Physical Society, California Institute of Technology, [www.zyvex.com/nanotech/feynman.html](http://www.zyvex.com/nanotech/feynman.html), July 13, **2006**
49. Drexler, K.E., "Engines of Creation", Anchor Press, New York, **1986**.
50. Desai, T.A.; Chu, W.H.; Tu, J.K.; Beattie J.M; Hayek A, Ferrari, M., *Biotechnol Bioeng*, **1998**, 57,118.
51. Leoni, L.; Desai, TA., *IEEE Trans Biomed Eng* **2001**, 48, 1335.
52. Lee, SB.; Martin, CR., *J Am Chem Soc* **2002**,124,11850.
53. Nishizawa, M.; Menon, VP.; Martin, CR.; *Science* **1995**, 268, 2.
54. Trofin, L.; Lee, SB.; Mitchell, D.T., *J Nanosci Nanotechnol* **2004**, 4, 239.
55. Martin, C.R.; Kohli, P.T., *Nature Rev Drug Discovery* **2003**, 2, 29.
56. Bayley, H.; Martin CR., *Chem Rev*, **2000**, 100,2575.
57. Mitchell, DT.; Lee, SB.; Trofin, L.; Li, N.; Nevanen, TK., *J Am Chem Soc* **2002**,124, 11864.
58. Harris, JM.; Martin, NE.; Modi, M., **2001**, 40, 539.
59. Kubo, T. ; Sugita, T.; Shimose, S. ; Nitta, Y.; Ikuta, Y.; Murakami T., *Int J Oncol*, **2000**, 17, 309.
60. Wust, P.; Hildebrandt, Sreenivasa B.; Rau,B. ; Gellermann, J; Riess H, *Lancet Oncol*, **2002**, 3, 487.
- 61.** Johannsen M, Gneveckow U, Thiesen B, Taymoorian K, Cho CH, Waldofner N. et al. *Eur Urol*. Published online at <http://www.sciencedirect.com> and at <http://www.ncbi.nlm.nih.gov>.

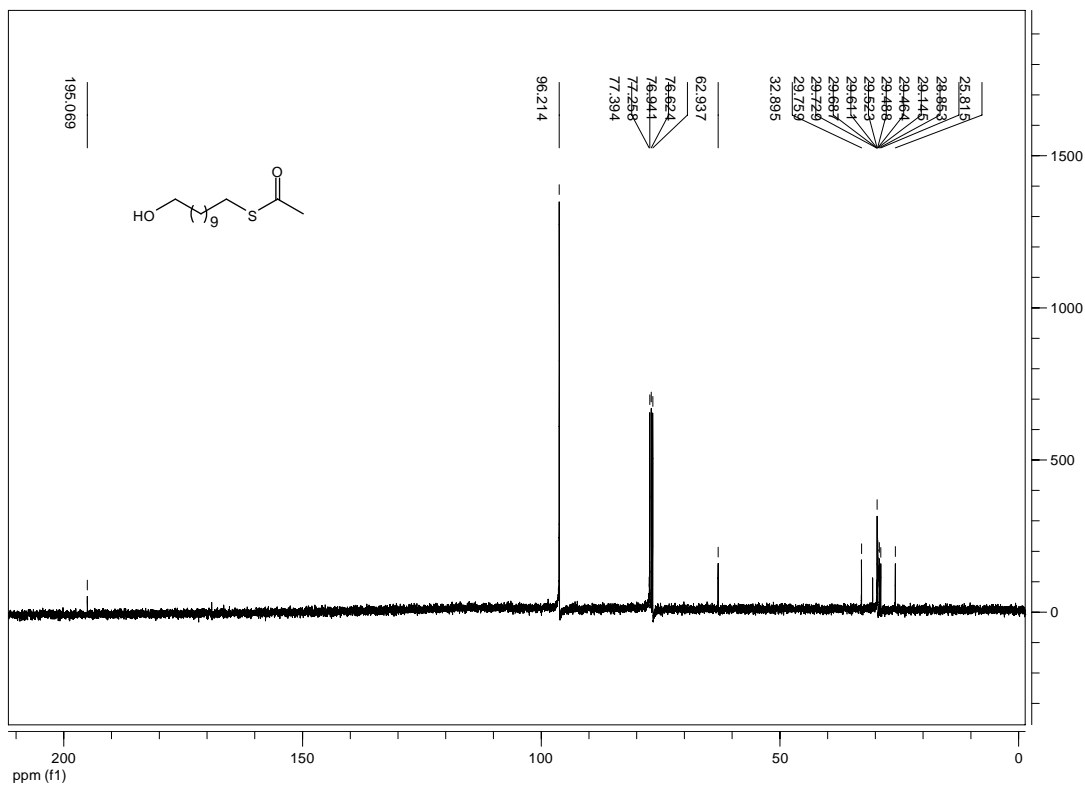
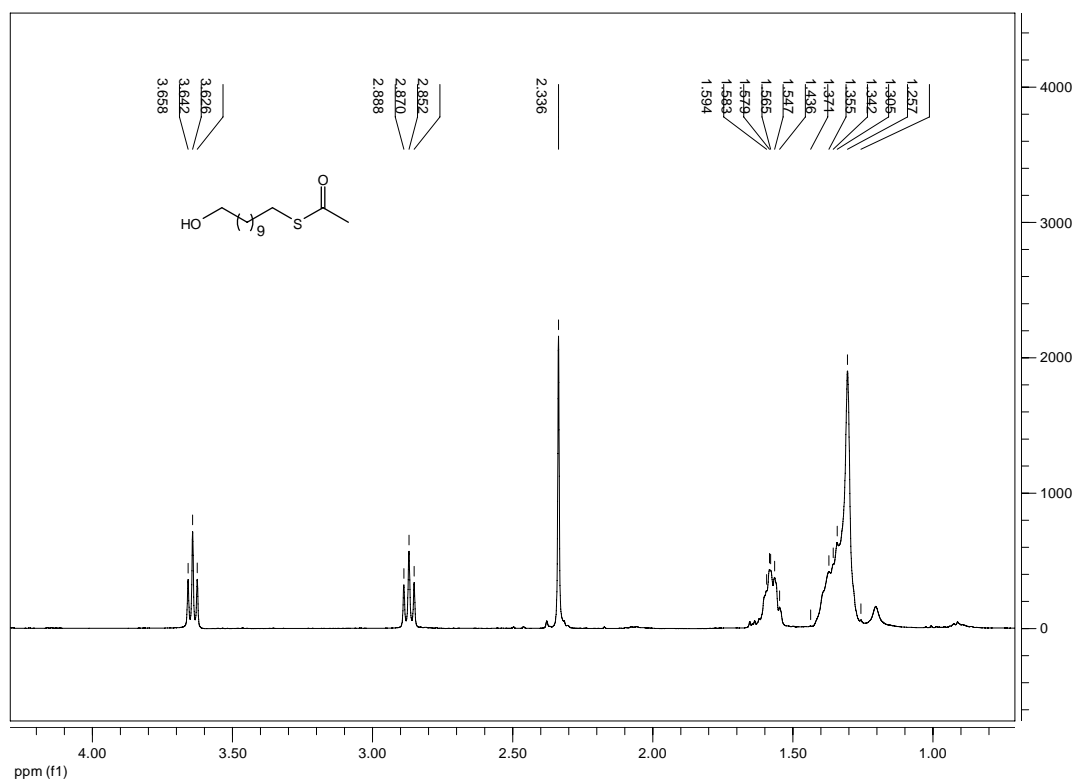
62. Meller, A.; L. Nivon,; Brandin, E.; Golovchenko, J.; Branton, D.; *Proc Natl Acad Sci USA*, **2002**, 97, 1079.
63. Meller A.; Nivon, L.; Branton, D., *Phys Rev Lett*, **2001**, 86, 3435.
64. Meller, A.; Branton, D., *Electrophoresis* **2002**, 23, 2583.
65. Deamer, D.W. ; Branton, D. ; *Acc Chem Res*, **2002**, 35, 817.
66. Branton, D. ; Meller, A., *Structure and dynamics of confined polymers*, **2002**, 177.
67. Wang. H. ; Branton, D. ; *Nature Biotechnol*, **2001**, 19, 622.
68. Li, J.; Gershow, M.; Stein, D.; Brandin, E.; Golovchenko, J.A., *Nat Materials*, **2003**, 2, 611.
69. Li, J.; Stein, D. ; McMullan, C. ; Branton, D. ; Aziz, M.J. ; Golovchenko, J.A. ; *Nature*, **2001**, 412, 166.
70. Stein, D.; Li, J.; Golovchenko, J.A. ; *Rev Lett*, **2002**, 89, 276.
71. Storm, A.J.; Chen, J.H.; Ling, X.S.; Zandbergen, H.W.; Dekker, C., *Nat Materials*, **2003**, 2, 537.
72. Chen, P.; Mitsui, T.; Farmer, D.B.; Golovchenko, J.; Gordon, R.G.; Branton, D., *Nano Lett*, **2004**, 4, 1333.
73. Sauer-Budge, A.F.; Nyamwanda, J.A.; Lubensky, D.K.; Branton, D. ; *Phys Rev Lett*, **2003**, 90, 238, 101-1-4.
74. Deamer, D.W.; Akeson, M.; *Trends Biotechnol*, **2000**, 18, 147.
75. Schinazi, R.F. ; Sijbesma, R. ; Srdanov, G. ; Hill, C.L. ; Wudl, F. ; *Antimicrob Agents Chemother*, **1993**, 37, 170.
76. Tsao, N. ; Kanakamma, P.P. ; Luh, T.Y. ; Chou, C.K. ; Lei, H.Y. ; *Antimicrob Agents Chemother*, **1999**, 43, 2273.
77. Tsao, N.; Luh, T.Y. ; Chou, C.K. ; Wu, J.J. ; Lin, Y.S. ; Lei, H.Y. ; *Antimicrob Agents Chemother*, **1999**, 45, 1788.
78. Bosi, S. ; Da Ros, T. ; Castellano, S. ; Banti, E. ; Prato, M. ; *Bioorg Med Chem Lett*, **2000**, 10, 1043.
79. Tabata, Y.; Murakami, Y.; Ikada, Y.; *Jpn J Cancer Res*, **1997**, 88, 1108.
80. Tabata, Y.; Murakami, Y.; Ikada, Y.; *Fullerene Sci Technol*, **1997**, 5, 989.
81. Miyata, N.; Yamakoshi, T.; *In: Kadish KM, Ruoff RS, editors. Society*, **1997**, 5, 345.

82. Dugan, LL.; Lovett, E. ; Cuddihy, S. Ma, B. ; Lin, T. ; Choi, DW. ; *Fullerenes: chemistry, physics, and technology*. New York: John Wiley; **2000**, 467.
83. Sessa, G.; *J. Clin. Invest.*, **1969**, 48, .
84. Bangham, A.D. *J. Mol. Biol.* **1965**, 13, 238.
85. Gabizon, A., *J. Control. Release*, **1998**, 53, 275.
86. Allen, T.M. , *Drugs*, **1997**, 4, 8.
87. Lasic, D.D. *Curr. Opin. Mol. Ther.* ,**1999**, 1, 177.
88. West, JL. ; Halas, NJ. ; *Curr Opin Biotechnol*, **2000**, 11, 215.
89. Sershen, SR.; Westcott, SL.; Halas, NJ. ; West, JL. ; *J Biomed Mater Res*, **2000**, 51, 293.
90. Pricl, S. ; Fermeglia, M. ; Ferrone, M. ; Asquini, A. ; *Carbon*, **2003**, 41, 2269.
91. Namazi, H. ; Adeli, M. ; *Biomaterials*, **2004**, 26, 1175.
92. Cloninger MJ. ; *Curr Opin Chem Biol* **2002**, 6, 742.
93. Hussain, M. ; Shchepinov, M.; Sohail, M. ; Benter, IF. ; Hollins, AJ. ;Southern, EM. ; *J Controlled Release*, **2004**, 99, 139.
94. Quintana, A. ; Raczka, E. ; Piehler, L. ; Lee, I. ; Myc, A. ; Majoros, I. ; *Pharm Res*, **2002**, 19, 1310.
95. Meijer, EW ; Van Genderen MHP, *Nature*, **2003**, 426, 128.
96. Kannan, S. ; Kolhe, P. ; Raykova, V. ; Glibatec, M.; Kannan, RM. ; Lieh-Lai M, *Biomat Sci Polymer Ed*, **2004**, 15, 311.
97. Jevprasesphant, R. ; Penny, J. ; Attwood, D. ; D'Emanuele, A. ; *J Controlled Release*, **2004**, 97, 259.
98. Neerman, MF, ; Zhang, W. ; Parrish, AR.; Simanek, EE., *Int J Pharm*, **2004**, 281, 129.
99. Tansey, W. ; Ke, S. ; Cao, XY. ; Pasuelo, MJ. ; Wallace, S. ; Li, C. ; *J Controlled Release*, **2004**, 94, 39.
100. Paleos, CM.; Tsiourvas, D. ; Sideratou, Z. ; Tziveleka, L. ; *Biomacromolecules*, **2004**, 5, 524 .
101. Sashiwa, H. ; Aiba, S-I. ; *Prog Polymer Sci*, **2004**, 29, 887.
102. Sun, Y.; Mayers, BT.; Xia, Y.; *Nano Lett*, **2002**, 2, 481.
103. Rfsler, A. ; Vandermeulen, GW. ; Klok, HA. ; *Adv Drug Delivery Rev*, **2001**, 53, 95.
104. Bagwe, RP. ; Zhao, X. ; Tan, W. ; *J Dispersion Sci Technol*, **2003**, 24, 453 .

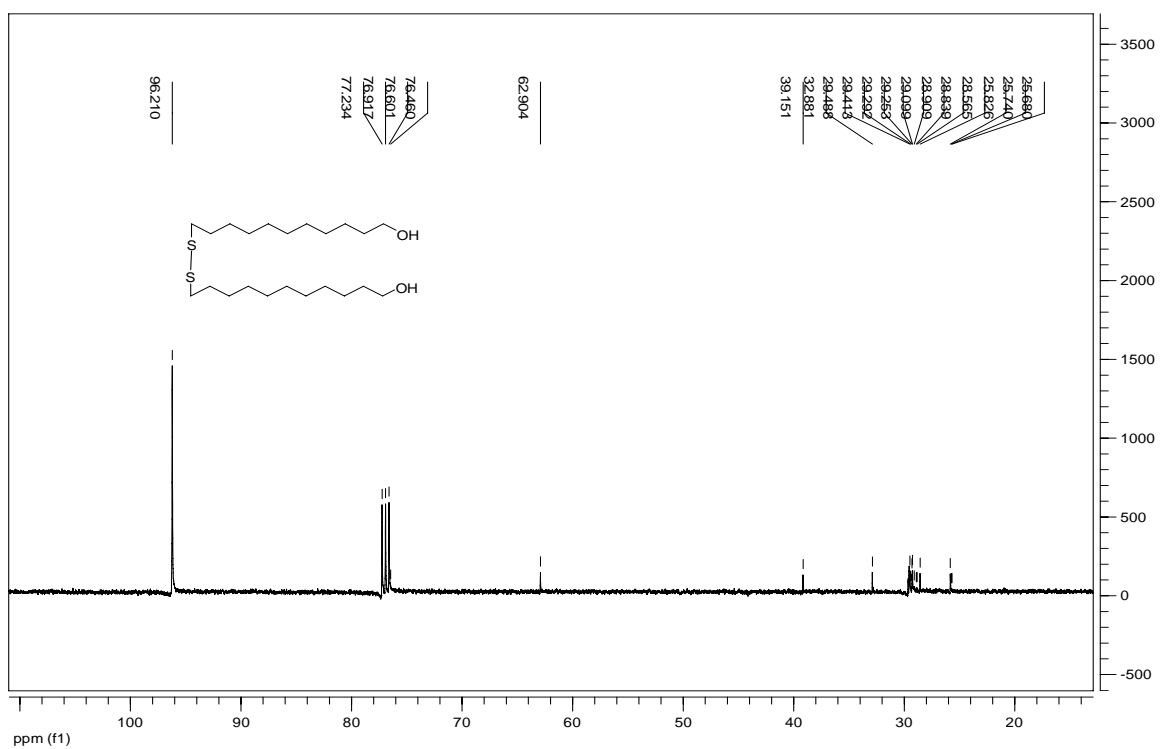
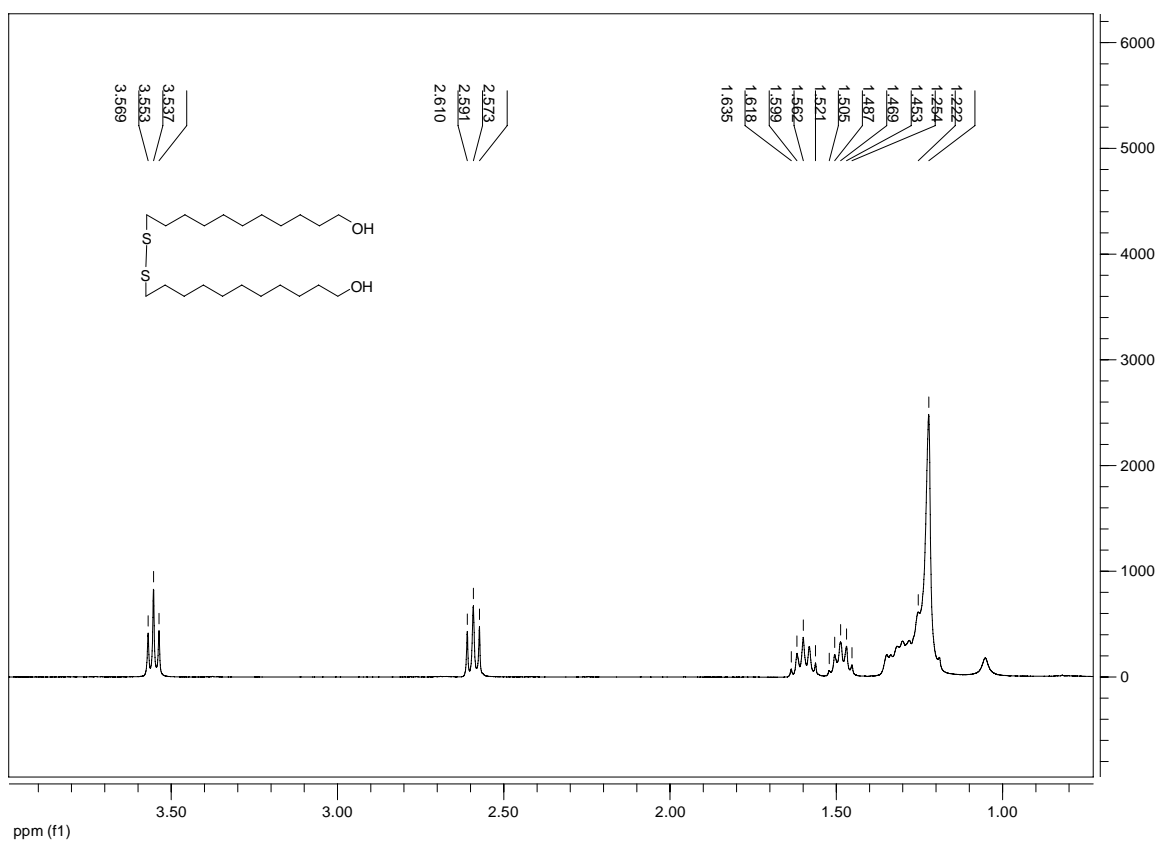
105. Rashid, M.H. ; Bhattacharjee, R.R. ; Kotal, A. ; Mandal, T.K. ; *Langmuir* , **2006**, 22, 7141.
106. Frens, G. ; *Nature Phys. Sci.*, **1973**, 241, 20.
107. Ullman, A.; *Chem. Rev.*, **1996**, 96, 1533.
108. Petit, C.; Lixon, P.; Pileni, M.; *J. Phys. Chem. B*, **1993**, 97, 129.
109. Suslick, K.S.; Fang, M.; Hyeon, T.; *J. Am. Chem. Soc.*, **1996**, 118, 11960.
110. Feldheim, D.L.; Keating, C.D. ; *Chem. Soc. Rev.*, **1998**, 27, 1.
111. Wall, M. E.; Wani, M. C.; Cook, C. E. ; Palmar, K. H. ; McPhail, A. T. ; Sim, G. A. ; *J. Am. Chem. Soc.*, **1966**, 88, 3888.
112. (a) Fassberg, J. ; Stella, V. J. ; *J. Pharm. Sci.*, **1992**, 81, 676. (b) Burke, T. G. ; Mi, Z. ; *J. Med. Chem.*, **1994**, 37, 40. (c) Cao, Z. ; Harris, N. ; Kozielski, A. ; Vardeman, D. ; Stehlin, J. S. ; Giovanella, B. ; *J. Med. Chem.*, **1998**, 41, 31.
113. Cao, Z.; *Synthetic Commun*, **1997**, 27, 2013.
114. Fassberg, J.; Stella, J. V.; *J. Pharm. Sci.*, **1992**, 81, 676.
115. Hertzberg, R. P.; Caranfa, M. J.; Holden, K. G.; Jakas, D. R.; Gallagher, G.; Mattern, M. R.; Mong, S. M.; Bartus, J. O.; Johnson, R. K.; Kingsbury, W. D. *J. Med. Chem.*, **1989**, 32, 715.
- 116(a) Nicholas, A. W.; Wani, M. W.; Manikumar, G.; Wall, M. E.; Kohn, K. W.; Pommier, Y. *J. Med. Chem.*, **1990**, 33, 972; (b) Wang, X.; Zhou, X.; Hecht, S. M. *Biochemistry*, **1999**, 38, 4374; (c) Emerson, D. L.; Burke, T. G. *Pharm. Sci. Tech. Today*. **2002**, 3, 205; (d) Yang, S. C.; Zhu, J. B. *Drug Develop. Indust. Pharm.*, **2002**, 28, 265.
117. Vishnuvajjala, B. R.; Garzon-Aburbeh, A. *U.S. Patent*, **1990**, 4, 943, 579.
- 118 (a) Cao, Z.; Harris, N.; Kozielski, A.; Vardeman, D.; Stehlin, J. S.; Giovanella, B. *J. Med. Chem.*, **1998**, 41, 31; (b) Cao, Z.; Pantazis, P.; Mendoza, J.; Early, J.; Kozielsky, A.; Harris, N.; Vardeman, D.; Liehr, J.; Stehlin, J. S.; Giovanella, B. *Ann, N. Y. Acad. Sci*, **2000**, 992, 122 (c) Yang, L.-X.; Pan, X.; Wang, H.-J. *Bioorg. Med. Chem. Lett.*, **2002**, 12, 1241.
119. Rahier, N. J.; Eisenhauer, B. M.; Gao, R.; Jones, S. H. Hecht, S. M., *Org. Lett.*, **2004**, 6(3), 321.
120. Zhao, H.; Lee, C.; Sai, P.; Choe, Y. H.; Boro, M.; Pendri, A.; Guan, S.; Greenwald, R. B., *J. Org. Chem.*, **2000**, 65, 4601.

121. Svarovskya, S. A. ; Szekelyb, Zoltan ; J. J. ;Barchi, Jr; *Tetrahedron: Asymmetry*, **2005**, 16 , 587.
122. Edwards, P. P. ; *Mat. Res. SOC. Symp. Proc.*, **1992**, 272, 311 .
123. Turkevich, J.; *Disc. Faraday Soc.*, **1951**, 11, 55.
124. Brust, M.; Walker, M. ; Bethell, D. ; Schiffrin, D. J. ; Whyman, R. ; *J. Chem. Soc., Chem. Comm.*, **1994**,. 801.
125. Cunnane, V. J. ; Schiffrin, D. J. ; Beltran, Geblewicz, C. G.; Solomon, T. ; *J. Electroanal. Chem.*, **1988**, 247, 103.

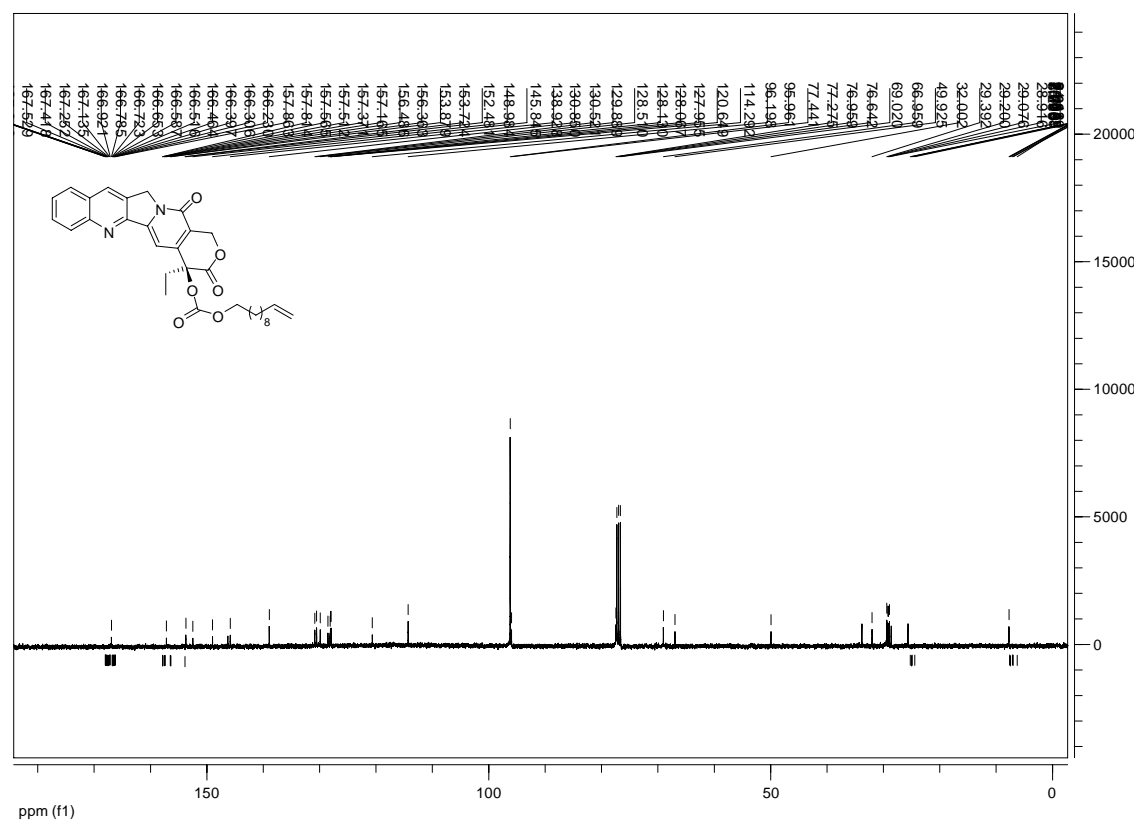
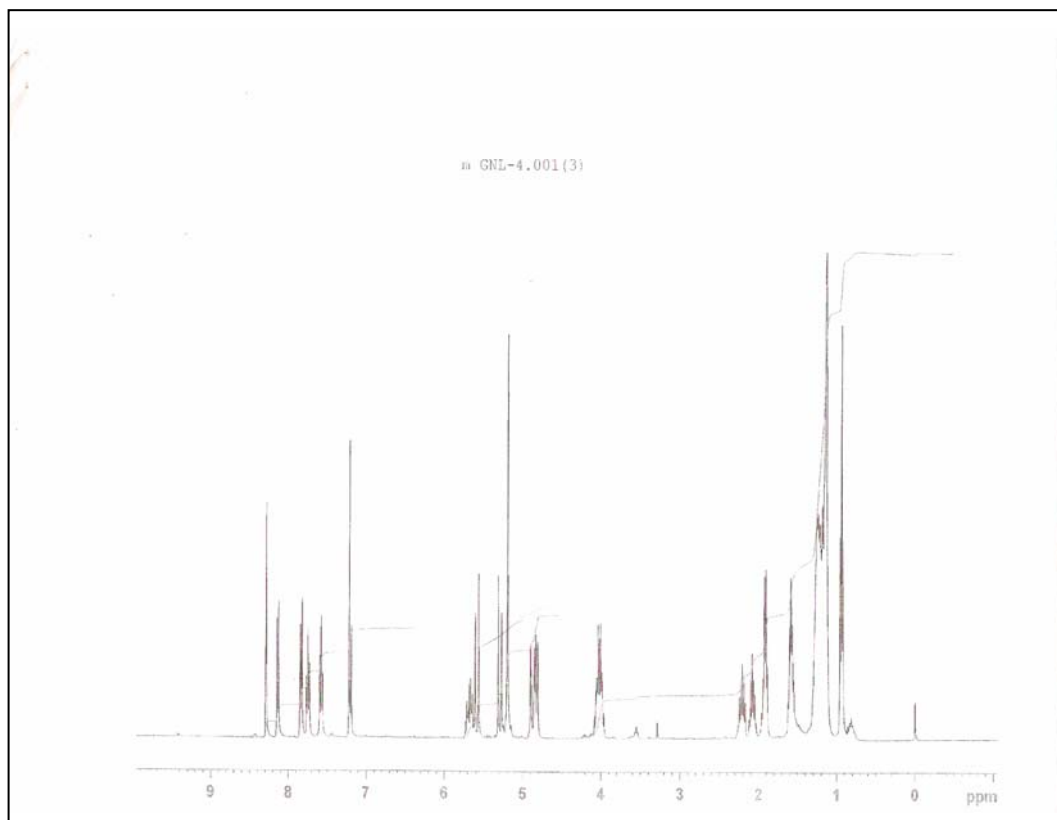
## APPENDIX



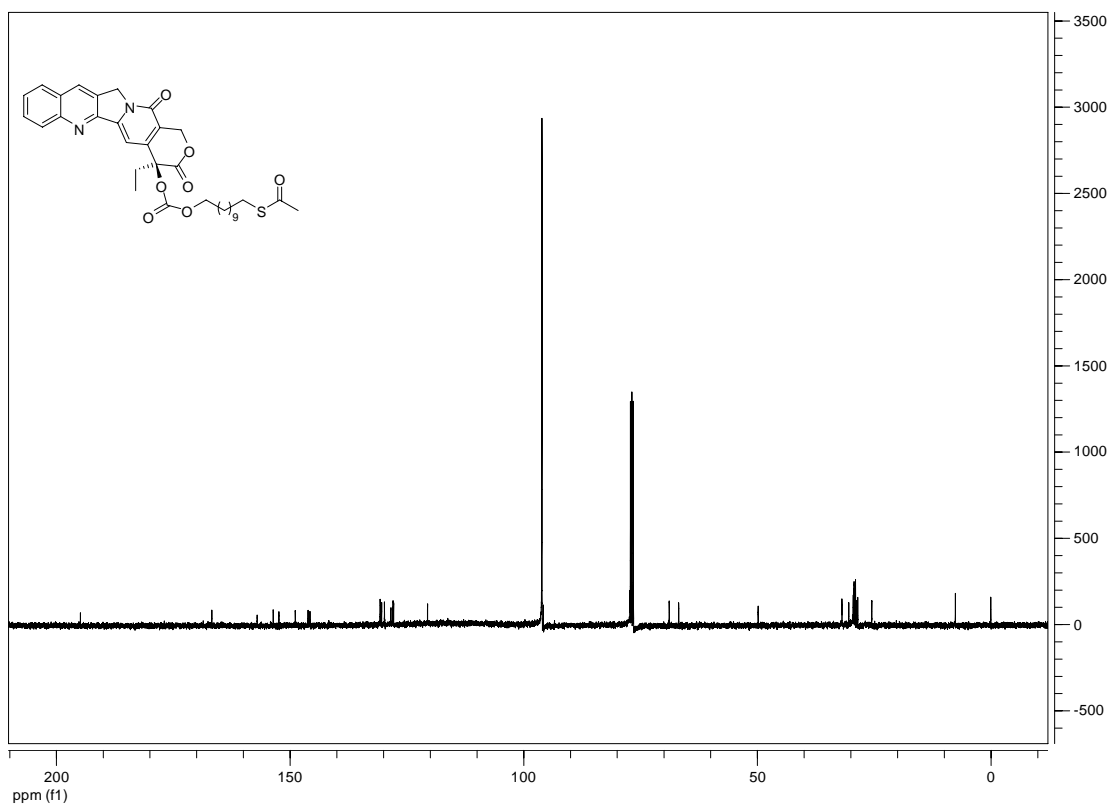
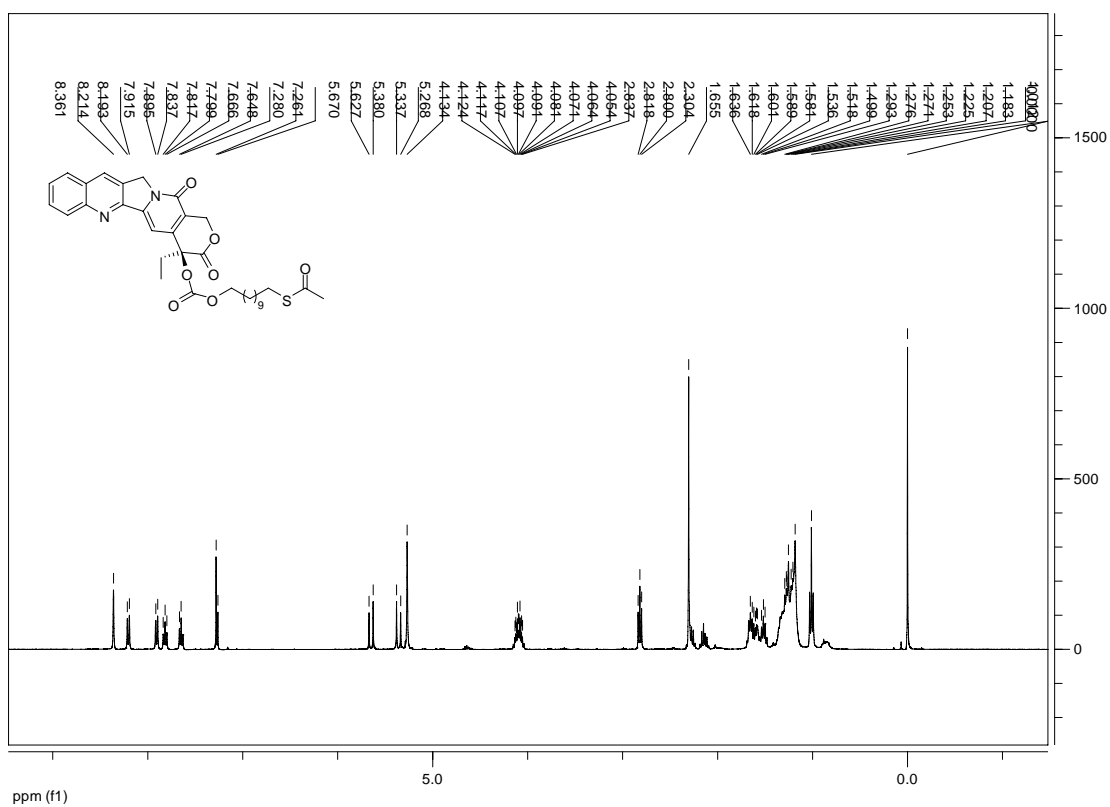
**Figure 32:** <sup>1</sup>H and <sup>13</sup>C NMR spectra of (6)



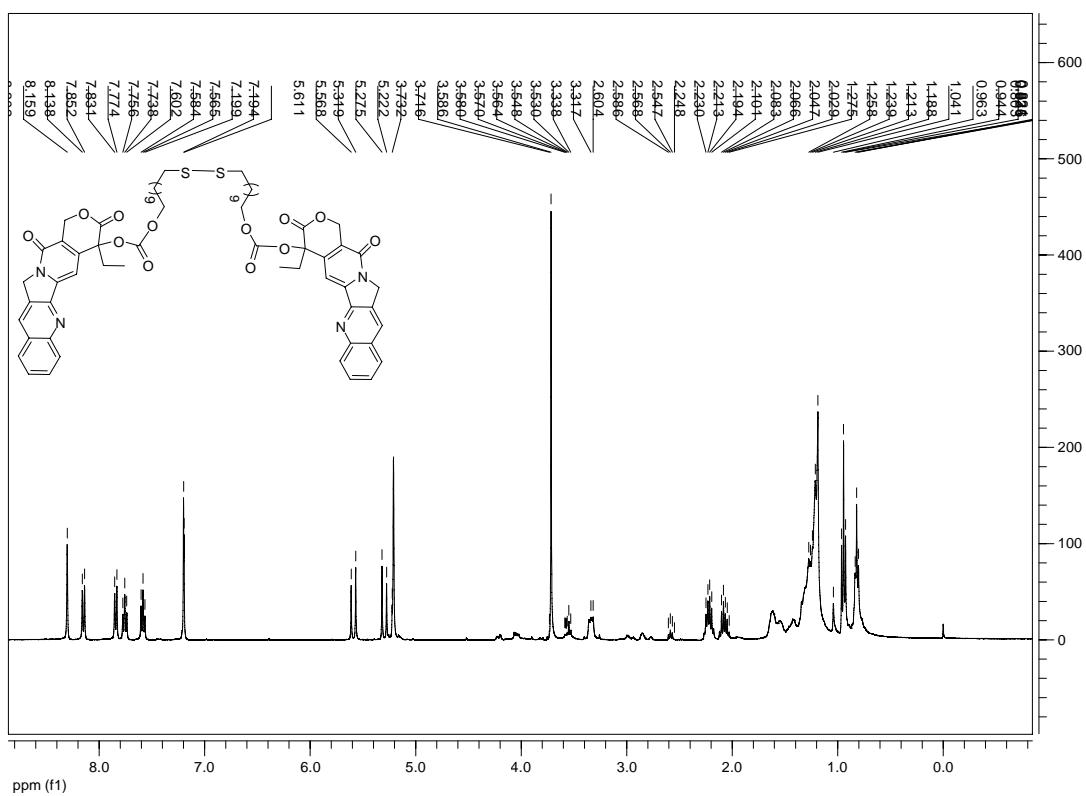
**Figure 33:**  $^1\text{H}$  and  $^{13}\text{C}$  NMR spectra of (7)



**Figure 34 :**  $^1\text{H}$  and  $^{13}\text{C}$  NMR spectra of (15)



**Figure 35:** <sup>1</sup>H and <sup>13</sup>C NMR spectra of (17)



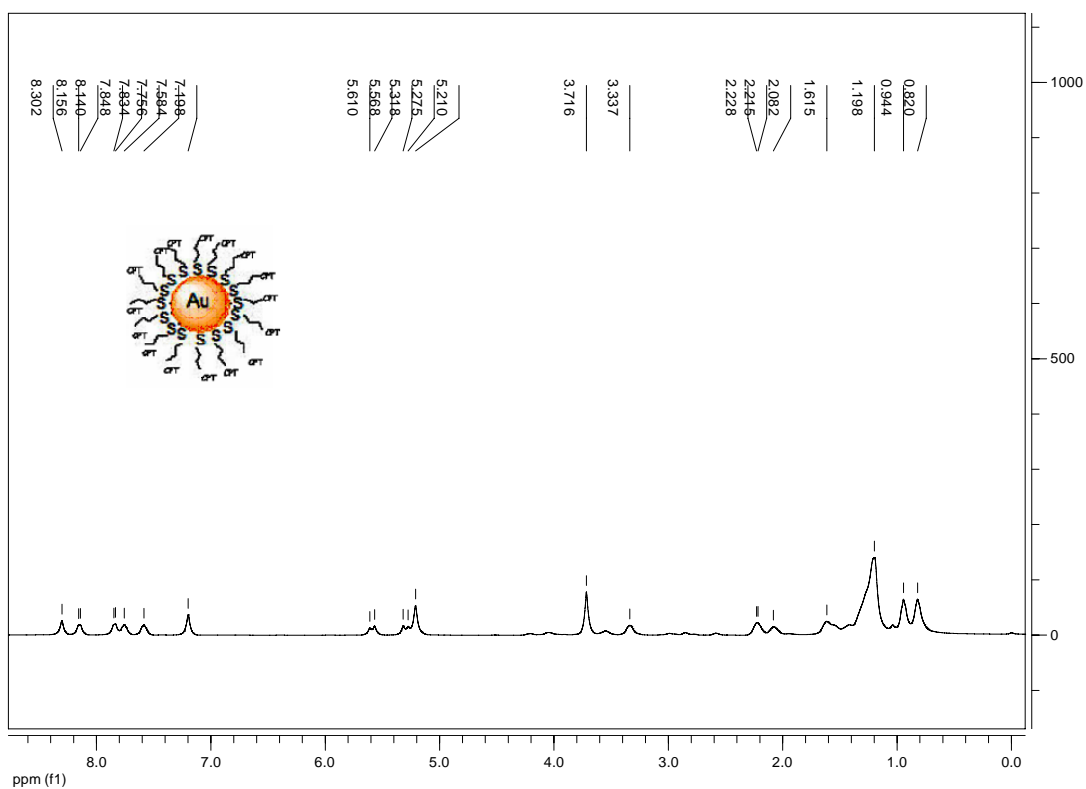


**Figure 37:**  $^1\text{H}$  spectra of 20-(11, 11'-disulfaneyldiundecan) - camptothecin Derivative coated Gold Nanoparticles